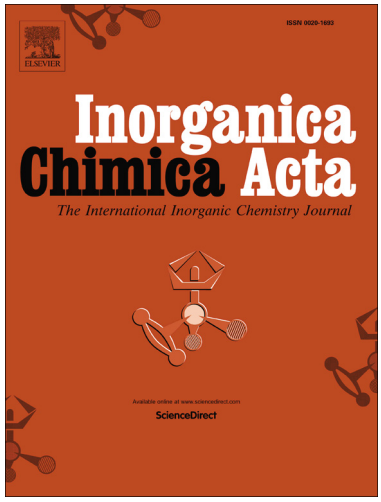


# Ruthenium(II)-Arene Complexes with Naphthalimide-Tagged N,O-and N, N-Chelating Ligands: Synthesis and Biological Evaluation

Kesete Ghebreyessus, Ashley Peralta, Meena Katdare, Krishnan Prabhakaran, Shanthi Paranawithana

PII: S0020-1693(15)00287-X
DOI: http://dx.doi.org/10.1016/j.ica.2015.05.025
Reference: ICA 16555

To appear in: *Inorganica Chimica Acta*

Received Date: 24 January 2015
Revised Date: 26 May 2015
Accepted Date: 28 May 2015

Please cite this article as: K. Ghebreyessus, A. Peralta, M. Katdare, K. Prabhakaran, S. Paranawithana, Ruthenium(II)-Arene Complexes with Naphthalimide-Tagged N,O-and N, N-Chelating Ligands: Synthesis and Biological Evaluation, *Inorganica Chimica Acta* (2015), doi: http://dx.doi.org/10.1016/j.ica.2015.05.025

# Ruthenium(II)-Arene Complexes with Naphthalimide-Tagged N,O-and N, N-Chelating Ligands: Synthesis and Biological Evaluation

Kesete Ghebreyessus[a]* Ashley Peralta[a#], Meena Katdare[b] Krishnan Prabhakaran[b#], Shanthi Paranawithana[a]

[a]Department of Chemistry and [b] Skin of Color Research Institute, Hampton University, Hampton, VA 23668

[a]* Corresponding Author: Kesete Ghebreyessus, Department of Chemistry, Hampton University, Hampton, VA 23666, USA. E-mail: Kesete.Ghebreyessus@hamptonu.edu. Telephone: +1-757-727-5475, Fax: +1-757-727-5604.

## ABSTRACT

A new family of ruthenium(II)-arene complexes with naphthalimide functionalized N,O- and N,N-chelating ligands of the general formula [Ru($\eta^6$-*p*-cymene)Cl(**L**)] (**2b-4b**) (where: **L** = 4-[N-(2-((2-hydroxy-5-Br-phenyl)methyl imino)ethyl)]-N-butyl-1,8-naphthalimide (**2a**), 4-[N-(2-((2-hydroxy-5-Cl-phenyl)methyl imino)ethyl)]-N-butyl-1,8-naphthalimide (**3a**), and N-butyl-4-[N-(2-((2-hydroxy-5-$NO_2$-phenyl)methylimino)ethyl)]-N-butyl-1,8-naphthalimide (**4a**), and [Ru($\eta^6$-*p*-cymene) Cl(**L'**)]Cl (**8b-9b**) (where **L'** = N-(2,2'-dipyridylaminoethyl)-1,8-naphthalimide (**8a**) and N-(2,2'-dipyridylaminopropyl)-1,8-naphthalimide (**9a**) have been synthesized and characterized. The *in vitro* cytotoxic activities of the ligands (**2a, 9a**) and the complexes (**2b-4b**, and **8b-9b**) have been evaluated against the human melanoma skin cancer (CRL7687) and normal noncancerous (CA-M75) cell lines. All the compounds exhibit potent cytotoxic activities with $IC_{50}$ values of ~ 1μM or less but displayed variable selectivity. The compounds with N, O- ligands were found to be less selective than those containing N, N-chelating ligands. Notably, complex **9b** displayed the highest selectivity towards cancer cells over health cells. The interactions of the compounds with calf thymus DNA (CT-DNA) have also been investigated by UV-vis and fluorescence spectra, ethidium bromide displacement assay and gel electrophoretic studies, which revealed that the compounds bind to CT-DNA moderately presumably through an intercalative mode.

**Key Words:** Ruthenium(II)-arene complexes; antitumor activity; DNA-binding; Naphthalimide-tagged chelating ligands

## 1. INTRODUCTION

Ruthenium based coordination and organometallic complexes are increasingly gaining in importance as promising candidates for the design of new and more effective metal-based anticancer agents [1-6]. This interest is stimulated by the successful entry of two ruthenium(III) compounds, NAMI-A ([$H_2$im][*trans*-$RuCl_4$(S-dmso)-(Him)]; Him = imidazole, dmso = dimethyl sulfoxide) and KP1019 ([$H_2$ind][*trans*-$RuCl_4(Hind)_2$]; Hind = indazole), into clinical trials [7-10]. More recently, promising result in clinical studies of NKP-1339 ([Na][*trans*-$RuCl_4(Hind)_2$]; Hind = indazole), the sodium analogue of KP1019 has also illuminated further interest for the design and development of ruthenium(III) based coordination compounds as anticancer agents [11-12]. The most attractive profile of NKP-1339 is its high water solubility compared to KP1019. It has been established that ruthenium compounds exhibit low toxicities while maintaining high selectivity toward cancer cells *in vitro* and high efficacy against platinum-drug-resistant tumors [9-13]. The more selective activity of ruthenium compounds is believed to be due to their preferential accumulation in cancer cells and the ability of ruthenium to mimic iron in binding to biomolecules [3, 7, 9, 11-13]. Ruthenium compounds are also believed to have a biological mode of action that is significantly different from those of platinum-based drugs [9, 13-15]. Furthermore, the rich synthetic chemistry, diverse coordination geometries, redox accessible oxidation states, and favorable ligand substitution reactions of ruthenium complexes have been advantageously considered for the design of new anticancer agents [3, 16].

More recently, the family of half-sandwich ruthenium(II)-arene organometallic complexes are also being actively investigated and evaluated as a potential source of new and effective metal-based anticancer agents. A favorable property of this type of complexes is the versatile pseudo-tetrahedral coordination geometry conferred by the metal center. Such a characteristic provides considerable possibilities for creating new compounds with interesting biological properties through rational ligand design and functionalization. In this context, several promising families of ruthenium(II)-arene based complexes with diverse ligand frameworks have been synthesized, and evaluated for their antitumor activity against a broad spectrum of cancer cell lines. For example, ruthenium(II)-arene complexes of the type $[(\eta^6\text{-arene})Ru(en)Cl]^+$ (en = 1,2-ethylenediamine) developed by Sadler and co-workers have shown to exhibit high antitumor activities in various cancer cell-lines [16-21]. Related compounds of the type $[(\eta^6\text{-arene})RuCl_2(pta)]$ (pta = 1,3,5-triaza-7-phosphaadmantane) reported by the Dyson group have also been shown to exhibit antimetastatic and antitumor activities [1, 10, 22-25]. The antitumor activity of many ruthenium(II)-arene complexes is generally related to their enhanced DNA binding affinity, which involves covalent coordination and/or simultaneous intercalation of extended aromatic groups and specific hydrogen bonding depending on the particular type of ligands used. In this regard, diverse ligand types are increasingly being developed and combined with the ruthenium(II)-arene moiety to enhance their DNA-binding properties, so as to achieve different biological functions and to maximize their effectiveness as therapeutic agents [21-26].

In recent years, research on targeted and multifunctional ruthenium(II)-arene complexes tethered to biologically active ligands have received increasing attention,

mainly due to the potential synergism that could be achieved by combining a metal ion and a bioactive ligand [1, 27-30]. It has been noted that tethering of biologically active ligands to the metal ion increases the biological potency of the complexes, through a combination of increased solubility, altered mechanisms of action, increased uptake, and improved cancer targeting properties. Dyson and co-workers have recently prepared new half-sandwich ruthenium(II)-arene complexes that incorporate the bioactive 1,8-naphthalimde-tagged arene and imidazole based ligands and,-which exhibited significantly higher anticancer activities compared to the prototype [($\eta^6$-arene)$RuCl_2$(pta)] (pta = 1,3,5-triaza-7-phosphaadmantane) complexes. The higher cytotoxic activity of these new complexes is attributed to the incorporation of the 1,8-naphthalimide moiety onto the ruthenium(II)-arene unit, which provides multi-targeting properties including strong DNA-binding and interaction with proteins [29].

In light of these promising results, we initiated the investigations on the design and synthesis of new ruthenium(II)-arene complexes consisting of N,O- and N, N- based chelating ligands conjugated with the bioactive 1,8-naphthalimide moiety as potential anticancer agents. 1,8-naphthalimides are heterocyclic pharmacophores that are known to readily interact with DNA through intercalation, and also to act as potent topoisomerase II inhibitors [31-36]. As a result, 1,8-naphthalimide and its derivatives have been extensively investigated for their potential use as anticancer drugs, and two of these compounds (mitonafide, and amonafide) have reached clinical trials [32-34]. In addition to their broad spectrum of biological activities, 1,8-naphthalimides have also been described as strongly fluorescent agents, a property that could be useful for probing the interaction of these compounds with biomolecules [37-40].

Hence, in this article, we report the synthesis and characterization of a series of naphthalimide-tethered chelating ligands and their corresponding ruthenium(II)-arene complexes. The cytotoxic activity of the complexes toward the human skin melanoma cancer cell line (CRL7687) and normal skin melanocyte (CA-M75) was investigated by using the methylthiazolyldiphenyltetrazolium bromide (MTT) assay. The DNA-binding properties of the compounds were explored by UV-Vis and fluorescence spectroscopy, and gel electrophoretic mobility studies. The results of our investigation revealed that conjugation of the naphthalimide moiety to the ruthenium(II) center have no distinct advantages on the cytotoxic activities of the ruthenium(II)-arene complexes on the cell lines tested. The details are presented herein.

## 2. Experimental Section

### *2.1. Materials and Methods*

All synthetic procedures were performed under nitrogen. All chemicals and solvents were purchased from commercial sources and used as received. Double stranded calf thymus DNA (CT-DNA) (Sodium salt, highly polymerized type) and supercoiled pUC18 plasmid DNA were purchased from Sigma Aldrich. $[(\eta^6\text{-cymene})RuCl_2]_2$ was prepared according literature methods [41]. $^1H$ and $^{13}C\{^1H\}$ NMR spectra were recorded on a JEOL Eclipse2-400 MHz spectrometer using solvent resonances as internal references. Electrospray ionization (ESI) mass spectra were recorded on an Agilent (Varian) MS-500 series and analyzed using MS-Varian 6.9.3 software. UV-vis absorption spectra were recorded on a Varian Cary 50 BIO spectrometer and emission spectra on a Cary Eclipse fluorospectrometer. Milli-Q $H_20$ (18.2 mΩ) was used as a solvent for all UV-vis, fluorescence, and gel electrophoresis studies.

**2.2. Synthesis and characterization of the Ligands (2a-4a)**

*2.2.1. Synthesis of 4-[(2'-aminoethyl)amino]-N-butyl-1,8-naphthalimide (**1**)*

The precursor compound, 4-[(2'-aminoethyl)amino]-N-butyl-1,8-naphthalimide (**1**), was synthesized following a procedures reported in the literature [42-43].

*2.2.2. Synthesis of N-(2-((2-hydroxy-5-Br-phenyl)methylimino)ethyl)-N-butyl-1,8-naphthalimide (**2a**).*

A stirred solution of the precursor compound 4-[(2'-aminoethyl)amino]-N-butyl-1,8-naphthalimide (**1**), (0.50 g) and 5-Bromo-salicylaldehyde in ethanol (50 mL) was heated to reflux for 24 h under a nitrogen atmosphere. The volume of the reaction mixture was reduced to ~ 5 mL by rotary evaporation. The solution was then cooled to room temperature and placed in an ice bath to precipitate the product. The resulting yellow precipitate was isolated by filtration and washed with diethyl ether to give the pure product as a yellow microcrystalline solid (yield: 0.56 g, 71%).

Anal. Calcd. for $C_{25}H_{25}N_3O_3Br$: C, 60.61; H, 5.09; N, 8.48.Found: C, 60.43; H, 4.91; N, 8.50. ESI-MS ($CH_3CN$): m/z = 494.7 [**2a** + H]$^+$. $^1$H NMR ($CDCl_3$, 400 MHz) δ 8.58 (dd, J = 7.3 Hz, J = 0.9 Hz, 1H, Ar-H), 8.48 (d, J = 8.7 Hz,1H, Ar-H), 8.31 (s, CH=N), 8.03 (d, J = 7.8 Hz,1H, Ar-H), 7.62 (d, J = 7.3 Hz, 1H, Ar-H), 7.40 (dd, J = 6.4 Hz, J = 2.8 Hz, 1H, Ar-H), 7.32 (d, J = 2.3 Hz, 1H, Ar-H), 6.87 (d, J = 8.7 Hz, 1H, Ar-H), 6.81 (d, J = 8.2 Hz, 1H, Ar-H), 5.47 (t, J = 6.0 Hz, 1H, NH), 4.16 (t, J = 7.8 Hz, 2H, $NCH_2CH_2$-, butyl), 4.00 (t, J = 5.5 Hz, 2H,$NCH_2$-), 3.83 (q, J = 6.0 Hz, 2H, -$NCH_2CH_2$), 1.71 (m, 2H, -$CH_2CH_2CH_3$, butyl), 1.44 (m, 2H, -$CH_2CH_2CH_2$-, butyl), 0.92 (t, J = 7.4 Hz, 3H, $CH_3$, butyl). $^{13}$C ($CDCl_3$, 100 MHz) δ 166.0 (C=O), 164.6 (C=O), 164.1 (N=CH), 159.9 (Ar-C), 148.5 (Ar-C), 135.5 (Ar-C), 134.1 (Ar-C), 133.7 (Ar-C), 131.2 (Ar-C), 129.8 (Ar-C),

125.5 (Ar-C, Ph), 125.2 (Ar-C, Ph), 123.4 (Ar-C, Ph), 120.4 (Ar-C), 119.8 (Ar-C), 119.1 (Ar-C),111.4 (Ar-C), 110.4 (Ar-C), 104.6 (Ar-C), 57.9 ($NCH_2$-), 43.9 ($NCH_2$, butyl), 40.0 ($CH_2NH$), 30.3 ($NCH_2CH_2$-, butyl), 20.4 (-$CH_2CH_2CH_2$-), 13.9 ($CH_3$, butyl).

*2.2.2. Synthesis of N-(2-((2-hydroxy-5-Cl-phenyl)methylimino)ethyl)-N-butyl-1,8-naphthalimide (**3a**).*

The same procedure as in **2a** using 5-Chloro-salicylaldehyde to give **3a** (yield: 0.60 g, 83%). Anal. Calcd. for $C_{25}H_{25}N_3O_3Cl$: C, 66.59; H, 5.59; N, 9.32. Found: C, 66.40; 5.38; N, 9.20. ). ESI-MS ($CH_3CN$): m/z = 450.4 [**3a**]$^+$. $^1$H NMR ($CDCl_3$, 400 MHz) δ 8.58 (d, J = 7.3 Hz, 1H, Ar-H), 8.48 (d, J = 8.2 Hz, 1H, Ar-H), 8.31 (s, 1H, N=CH), 8.04 (d, J = 8.3 Hz, 1H, Ar-H), 7.61 (d, J = 7.3 Hz, 1H, Ar-H, Ph), 7.28 (d, J = 2.8 Hz, 1H, Ar-H), 7.17 (d, J = 2.8 Hz, 1H, Ar-H), 6.92 (d, J = 8.7 Hz, 1H, Ar-H, Ph), 6.81 (d, J = 8.3 Hz, 1H, Ar-H, Ph), 5.50 (t, J = 6.0 Hz, 1H, NH), 4.16 (t, J = 7.3 Hz, 2H, -$NCH_2CH_2$-, butyl), 4.00 (t, J = 6.0 Hz, 2H, -$CH_2N$), 3.83 (q, J = 5.5 Hz, 2H, $NHCH_2$), 1.71 (m, 2H, -$CH_2CH_2CH_2$-, butyl), 1.44 (m, 2H, -$CH_2CH_2CH_3$, butyl), 0.97 (t, J = 7.3 Hz, 3H, $CH_3$, butyl). $^{13}$C ($CDCl_3$, 100 MHz) δ 166.0 (C=O), 164.6 (C=O), 164.1 (C=NH), 159.9 (C-O), 148.5 (C-NH), 134.1 (Ar-C), 132.7 (Ar-C), 131.2 (Ar-C), 130.6 (Ar-C), 129.8 (Ar-C, Ph), 125.5 (Ar-C, Ph), 125.1 (Ar-C, Ph), 123.6 (Ar-C, Ph), 123.4 (Ar-C), 120.4 (Ar-C), 119.2 (Ar-C), 118.6 (Ar-C), 111.4 (Ar-C), 104.5 (Ar-C, Ph), 57.9 ($NCH_2$-), 43.9 (-$NCH_2$-, butyl), 40.0 (-$CH_2NH$-), 30.3 (-$CH_2CH_2$-, butyl), 20.4 (-$CH_2CH_3$, butyl), 13.9 ($CH_3$, butyl).

*2.2.3. Synthesis of N-(2-((2-hydroxy-5-$NO_2$-phenyl)methylimino)ethyl)-N-butyl-1,8-naphthalimide (**4a**).*

The same procedure as in **2a** using 5-nitro-salicyladehyde to give **4a** (yield: 0.52 g, 70%). Anal. Calcd. for $C_{25}H_{25}N_4O_5$: C, 65.08; H, 5.46; 12.14. Found: C, 64.92; H, 5.42; N, 19.93. ESI-MS ($CH_3CN$): m/z = 461.4 [**4a**]$^+$. $^1$H NMR ($CDCl_3$, 400 MHz) δ 8.65 (s, 1H, N=CH), 8.61 (d, J = 8.7 Hz, 1H, Ar-H), 8.41 (d, J = 6.8 Hz, 1H, Ar-H), 8.28 (dd, J = 8.7 Hz, J = 2.7 Hz, 1H, Ar-H), 8.14 (m, 1H, Ar-H, Ph), 8.01 (dd, J = 9.2 Hz, J = 2.8 Hz, 1H, Ar-H), 7.81 (t, J = 7.8 Hz, 1H, N-H), 7.61 (t, J = 7.8 Hz, 1H, Ar-H), 6.86 (d, J = 8.7 Hz, 1H, Ar-H, Ph), 6.67 (d, J = 9.6 Hz, 1H, Ar-H, Ph), 4.00 (m, 4H, $NCH_2$, ethyl; $NCH_2$-, butyl), 3.77 (q, J = 5.5 Hz, 2H, -$CH_2NH$), 1.58 (m, 2H, $NCH_2CH_2$-, butyl), 1.35 (m, 2H, -$CH_2CH_2CH_3$, butyl), 0.92 (t, J = 7.3 Hz, 3H, $CH_3$, butyl), $^{13}$C ($CDCl_3$, 100 MHz) δ 167.2 (C=O), 165.8 (C=O), 164.5 (N=CH), 164.0 (C-O), 148.4 (Ar-C, Ph), 139.5 (Ar-C), 134.0 (Ar-C), 131.2 (Ar-C), 129.7 (Ar-C), 128.2 (Ar-C), 127.9 (Ar-C), 125.6 (Ar-C, Ph), 125.2 (Ar-C, Ph), 123.3 (Ar-C, Ph), 120.4 (Ar-C), 118.3 (Ar-C), 117.2 (Ar-C), 111.4 (Ar-C), 104.4 (Ar-C, Ph), 57.2 (-$NCH_2$), 43.7 ($NCH_2CH_2CH_2$-, butyl), 40.0 (-$CH_2N$), 30.3 (-$CH_2CH_2N$-, butyl), 20.4 (-$CH_2CH_2CH_2$-, butyl), 13.9 ($CH_3$, butyl).

**3. Synthesis of the 2,2'-dipyridylamine containing ligands (8a, 9a)**

*3.1.* Synthesis of *N-(2,2'-dipyridylaminoethyl)-1,8-naphthalimide (**8a**)*

The second series of ligands were synthesized using the following general procedure [44]. Under nitrogen, solutions of N-(1-bromoethyl)-1,8-naphthalimide (**7**) (0.305 g, 1.0 mmol) and 2,2'-dipyridylamine (0.20 g, 1.1 mmol) were suspended in acetonitrile. To this suspension, $Cs_2CO_3$ (0.36 g, 1.1 mmol) was added with stirring. The resulting mixture was refluxed for 24 h under nitrogen. The solution was cooled to room

temperature and the solvent was removed under reduced pressure. The resulting residue was dissolved in $CH_2Cl_2$ and layered with diethyl ether to precipitate the product. The precipitate was collected by filtration as a pale yellow solid: (yield: 0.35 g, 88%). Anal. Calcd. for $C_{24}H_{18}N_4O_2$: C, 73.09; H, 4.60; N, 14.21. Found: C, 73.49; H, 4.75; N, 14.09. ESI-MS ($CH_3CN$): m/z = 395.1 [**8a** + H]$^+$. $^1$H NMR ($CDCl_3$, 400 MHz) δ 8.60 (d, J = 7.3 Hz, 2H, Ar-H, Py), 8.26 (d, J = 5.0 Hz, 2H, Ar-H, Py), 8.22 (d, J = 8.2 Hz, 2H, Ar-H), 7.75 (t, J = 7.8 Hz, 2H, Ar-H), 7.59 (m, 4H, Ar-H, Py), 6.84 (t, J = 6.0 Hz, 2H, Ar-H, Py), 4.47 (t, J = 5.0 Hz, 2H, -$NCH_2$), 4.00 (t, J = 5.5 Hz, 2H, -$CH_2$N-).$^{13}$C NMR ($CDCl_3$, 100 MHz) δ 165.1 (C=O), 153.9 (Ar-C, Py), 147.7 (Ar-C), 137.7 (Ar-C), 134.2 (Ar-C), 131.5 (Ar-C), 128.2 (Ar-C), 126.9 (Ar-C), 122.4 (Ar-C), 116.4 (Ar-C), 111.6 (Ar-C), 61.7 (-$NCH_2$), 42.8 (-$CH_2$N-).

*3.2.* Synthesis of *N-(2,2'-dipyridylaminopropyl)-1,8-naphthalimide (**9a**)*

*T*he same experimental procedure as reported for **8a** (yield: 0.40 g, 85%). Anal. Calcd. for $C_{25}H_{20}N_4O_2$ 408.4: C, 73.51; H, 4.93; N, 13.62. Found: C, 73.30; H, 5.03; N, 13.54. ESI-MS ($CH_3CN$): m/z = 408.3 [**9a**]$^+$. $^1$H NMR ($CDCl_3$, 400 MHz) δ 8.60 (d, J = 7.3 Hz, 2H, Ar-H, Py), 8.26 (d, J = 5.0 Hz, 2H, Ar-H), 8.21 (d, J = 8.2 Hz, 2H, Ar-H), 7.75 (t, J = 7.8 Hz, 2H, Ar-H), 7.56 (m, 4H, Ar-H, Py), 6.84 (t, J = 6.0 Hz, 2H, Ar-H, Py), 4.33 (t, J = 7.3 Hz, 2H,-$NCH_2CH_2$), 3.50 (t, J = 6.9 Hz, 2H, -$CH_2CH_2$N), 2.33 (m, 2H, -$CH_2CH_2CH_2$-).$^{13}$C ($CDCl_3$, 100 MHz) δ 164.2 (C=O), 154.0 (Ar-C, Py), 147.8 (Ar-C), 137.8 (Ar-C), 134.1 (Ar-C), 131.6 (Ar-C), 131.4 (Ar-C), 128.2 (Ar-C), 127.0 (Ar-C), 122.5 (Ar-C), 116.4 (Ar-C), 111.6 (Ar-C), 39.3 ($NCH_2CH_2$-), 31.4 (-$CH_2CH_2$N-), 30.6 (-$CH_2CH_2$).

## 4. Synthesis and Characterization of the ($\eta^6$-*p*-cymene)ruthenium(II) complexes (2b-4b)

### *4.1. Synthesis of ($\eta^6$-p-cymene)(N-(2-((2-hydroxy-5-Br-phenyl)methylimino)ethyl)-N-butyl-1,8-naphthalimide)chlororuthenium(II) (**2b**)*

The ruthenium(II)-cymene complexes were synthesized following a similar procedure described in the literature, but with a slight modification [45]. The N-(2-((2-hydroxy-5-Br-phenyl) methylimino)ethyl)-N-butyl-1,8-naphthalimide ligand (**2a)** (0.25 g, 0.56 mmol) was dissolved in 25 mL of dry $CH_2Cl_2$, and K-O$^t$Bu (0.15 g, 0.56 mmol) was added at room temperature. The mixture was stirred for 30 min at room temperature. After the suspension was cooled in an ice bath, [($\eta^6$-*p*-cymene) $RuCl_2]_2$ (0.15 g, 0.25 mmol) was added. The solution was stirred for 24 h in an ice bath. The mixture was filtered through a short pad of Celite to remove insoluble materials. The volume of the filtrate was reduced to ~5 mL by rotary evaporation and the product was precipitated by the addition of hexane. The precipitate was isolated via filtration, washed with diethyl ether and air dried to give the products as a dark red solid: (yield: 0.50 g, 82%). Anal. Calcld. for $C_{35}H_{37}N_3O_3ClBrRu$: C, 55.02; H, 4.88, N, 5.50. Found: C, 54.94; H, 4.72; N, 5.40. ESI-MS ($CH_3CN$): m/z = 728.4 [($\eta^6$-*p*-cymene)Ru(**2a**)–Cl]$^+$. $^1$H NMR ($CDCl_3$, 400 MHz) $\delta$ 8.50 (d, J = 7.3 Hz, 1H, Ar-H), 8.45 (d, J = 8.2 Hz, 1H, Ar-H), 8.06 (d, J = 8.7 Hz, 1H, Ar-H), 7.41 (d, J = 7.8 Hz, 1H, Ar-H), 7.15 (d, J = 2.8 Hz, 1H, Ar-H), 7.13 (d, J = 2.8 Hz, 1H, Ar-H), 7.07 (s, 1H, HC=N), 6.78 (d, J = 9.2 Hz, 1H, Ar-H), 6.71 (d, J = 8.2 Hz, 1H, Ph), 5.57 (d, J = 6.4 Hz, 1H, *p*-cymene), 5.52 (d, J = 6.4 Hz, 1H, *p*-cymene), 5.43 (d, J = 5.5 Hz, 1H, *p*-cymene), 5.01 (d, J = 5.5 Hz, 1H, *p*-cymene), 4.51 (m, 1H, $NCH_2$), 4.26 (m, 2H, -$CH_2$NH), 4.16 (t, J = 7.3 Hz, 2H, -$NCH_2CH_2$-, butyl), 3.94 (m, 1H, $NCH_2$), 2.74 (sept, J = 6.9 Hz, 1H, $CH(CH_3)_2$, *p*-cymene), 2.30 (s, 3H, $CH_3$, *p*-cymene), 1.71 (m,

2H, $CH_2$, butyl), 1.44 (m, 2H, $CH_2$, butyl), 1.25 (d, J = 6.9 Hz, 3H, $CH(CH_3)$, *p*-cymene), 1.15 (d, J = 6.9 Hz, 3H, $CH(CH_3)$, *p*-cymene), 0.96 (t, J = 7.3 Hz, 3H, $CH_3$, butyl). $^{13}C$ ($CDCl_3$, 100 MHz) δ 164.7 (C=O), 164.3 (C=O), 164.0 (N=CH), 149.0 (C-O), 137.9 (Ar-C), 135.9 (Ar-C), 134.0 (Ar-C), 131.6 (Ar-C), 130.0 (Ar-C), 127.8 (Ar-C), 125.2 (Ar-C, Ph), 124.0 (Ar-C, Ph), 122.6 (Ar-C, Ph), 120.5 (Ar-C), 119.2 (Ar-C), 110.5 (Ar-C), 104.8 (Ar-C), 103.4 (Ar-C, Ph), 100.8 (Ar-C, Ph), 99.2 (Ar-C, *p*-cymene), 88.7 (Ar-C, *p*-cymene), 83.3 (Ar-C, *p*-cymene), 80.7 (Ar-C, *p*-cymene), 80.5 (Ar-C, *p*-cymene), 66.7 ($NCH_2$), 42.2 ($-CH_2NH$), 39.9 ($N-CH_2CH_2$, butyl), 30.7 ($CHCH_3$, *p*-cymene), 30.3 ($CH_2CH_2$, butyl), 23.0 ($CH_3$, *p*-cymene), 21.7 ($CH_2CH_2$, butyl), 20.5 ($CH_3$, *p*-cymene), 18.9 ($CH_3$, *p*-cymene), 13.9 ($CH_3$, butyl).

*4.2. Synthesis of (η6-p-cymene)(N-(2-((2-hydroxy-5-Cl-phenyl)methylimino)ethyl)-N-butyl-1,8-naphthalimide)chlororuthenium(II) (**3b**)*

The same experimental procedure as reported for **2b**, was employed using ligand **3a** to give **3b** as a red solid (yield: 0.50 g, 75%). Calcd. for $C_{35}H_{37}N_3O_3Cl_2Ru$: C, 58.41; H, 5.18; N, 5.84. Found: C, 58.11; H, 5.10; N, 5.54. ESI-MS ($CH_3CN$): m/z = 684.4 [($\eta^6$-*p*-cymene)Ru(**3a**)–Cl]$^+$. $^1H$ NMR ($CDCl_3$, 400 MHz) δ 8.51 (d, J = 7.4 Hz, 1H, Ar-H), 8.46 (d, J = 8.2 Hz, 1H, Ar-H), 8.08 (d, J = 8.7 Hz, 1H, Ar-H), 7.42 (t, J = 7.8 Hz, 1H, Ar-H), 7.10 (s, 1H, N=CH), 7.02 (dd, J = 9.2 Hz, J = 2.8 Hz, 1H, Ar-H), 6.84 (d, J = 9.2 Hz, 1H, Ar-H, Ph), 6.76 (m, 1H, N-H), 6.72 (d, J = 8.3 Hz, 1H, Ar-H, Ph), 6.20 (d, J = 2.8 Hz, 1H, Ar-H, Ph), 5.57 (d, J = 6.4 Hz, 1H, *p*-cymene), 5.52 (d, J = 6.0 Hz, 1H, *p*-cymene), 5.43 (d, J = 6.6 Hz, 1H, *p*-cymene), 5.00 (d, J = 5.5 Hz, 1H, *p*-cymene), 4.52 (m, 1H, $-NCH_2$), 4.27 (m, 2H, $-CH_2NH$), 4.16 (t, J = 7.4 Hz, 2H, $-NCH_2-$, butyl), 3.95 (m, 1H, $NCH_2-$), 2.75 (sept, J = 6.8 Hz, 1H, $CH(CH_3)_2$, *p*-cymene), 2.32 (s, 3H, $CH_3$, *p*-

cymene), 1.71 (m, 2H, $CH_2$, butyl), 1.44 (m, 2H, $CH_2$, butyl), 1.25 (d, J = 7.3 Hz, 3H, $CH(CH_3)$, *p*-cymene) 1.15 (d, J = 6.9 Hz, 3H, $CH(CH_3)$, *p*-cymene), 0.97 (t, J = 7.4 Hz, 3H, $CH_3$, butyl). $^{13}C$ ($CDCl_3$, 100 MHz) δ 164.7 (C=O), 164.3 (C=O), 163.7 (HC=N), 148.9 (C-O), 135.4 (Ar-C), 134.0 (Ar-C), 132.7 (Ar-C), 131.5 (Ar-C, *p*-cymene), 130.0 (Ar-C), 127.8 (Ar-C), 125.2 (Ar-C, Ph), 123.5 (Ar-C, Ph), 122.6 (Ar-C, Ph), 120.5 (Ar-C), 118.5 (Ar-C), 118.3 (Ar-C), 110.4 (Ar-C), 103.3 (Ar-C, Ph), 100.7 (Ar-C), 99.2 (Ru-C, *p*-cymene), 88.9 (Ru-C, *p*-cymene), 83.3 (Ru-C, *p*-cymene), 80.7 (Ru-C, *p*-cymene), 80.4 (Ru-C, *p*-cymene), 66.9 (-N-$CH_2$), 42.2 (-$CH_2$-NH), 40.0 (N-$CH_2CH_2$), 30.6 ($CH(CH_3)_2$, *p*-cymene), 30.3 (-$CH_2CH_2$, butyl), 23.0 ($CH_3$, *p*-cymene), 21.6 ($CH_2CH_2$, butyl), 20.5 ($CH(CH_3)$, *p*-cymene), 18.9 ($CH(CH_3)$, *p*-cymene), 13.9 ($CH_3$, butyl).

*4.3. Synthesis of ($\eta^6$-p-cymene)(N-(2-((2-hydroxy-5-$NO_2$-phenyl)methylimino)ethyl)-N-buthyl-1,8-naphthalimide)chlororuthenium(II) (**4b**)*

*T*he same experimental procedure as reported for **3b**, using ligand **4a** to give **4b** as an red-orange solid (yield: 0.50 g, 70%)**.** Anal. Calcd. for Calcd for $C_{35}H_{37}N_4O_5ClRu$: C, 57.57; H, 5.11; N, 7.67. Found: C, 57.89; H, 4.95; N, 7.55. ESI-MS ($CH_3CN$): m/z = 695.2 [($\eta^6$-*p*-cymene)Ru(**4a**)–Cl]$^+$. $^1H$ NMR ($CDCl_3$, 400 MHz) δ 8.46 (t, J = 7.8 Hz, 1H, Ar-H), 8.03 (d, J = 8.2 Hz, 1H, Ar-H), 7.95 (dd, J = 9.6 Hz, J = 2.7 Hz, 1H, Ar-H), 7.40 (t, J = 7.3 Hz, 1H, Ar-H), 7.32 (s, 1H, N=CH), 6.86 (d, J = 9.2 Hz, 1H, Ar-H), 6.71 (d, J = 8.2 Hz, 1H, Ar-H), 6.65 (m, 1H, Ar-H), 5.63 (d, J = 6.4 Hz, 1H, *p*-cymene), 5.59 (d, J = 6.4 Hz, 1H, *p*-cymene), 5.52 (d, J = 5.5 Hz, 1H, *p*-cymene), 5.06 (d, J = 6.0 Hz, 1H, *p*-cymene), 4.55 (m, 1H, -$NCH_2$), 4.29 (m, 2H, -$CH_2$NH-), 4.14 (t, J = 7.4 Hz, 1H, $NCH_2CH_2$-, butyl), 4.00 (m, 1H, -$NCH_2$), 2.76 (sept, J = 6.9 Hz, 1H, $CH(CH_3)_2$), *p*-cymene), 2.33 (s, $CH_3$, 3H, *p*-cymene), 1.71 (m, 2H, -$CH_2CH_2CH_2$-, butyl), 1.43 (m, 2H,

-$CH_2CH_2CH_3$), 1.26 (d, J = 6.8 Hz, 3H, $CH(CH_3)_2$, *p*-cymene), 1.17 (d, J = 6.9 Hz, 3H, $CH(CH_3)_2$, *p*-cymene), 0.95 (t, J = 7.3 Hz, 3H, -$CH_2CH_3$, butyl). $^{13}C$ ($CDCl_3$, 100 MHz) δ 170.1 (C=O), 165.1 (C=O), 164.5 (N=CH), 164.2 (C-O),148.6 (Ar-C), 135.7 (Ar-C), 134.0 (Ar-C), 132.7 (Ar-C), 131.5 (Ar-C), 130.0 (Ar-C), 129.6 (Ar-C),127.2 (Ar-C), 125.2 (Ar-C, Ph), 122.8 (Ar-C, Ph), 122.6 (Ar-C, Ph), 120.4 (Ar-C), 117.0 (Ar-C), 110.7 (Ar-C), 103.2 (Ar-C), 101.7 (Ar-C, Ph), 99.6 (Ar-C, Ph), 88.8 (Ar-C, *p*-cymene), 83.7 (Ar-C, *p*-cymene), 80.9 (Ar-C, *p*-cymene), 80.4 (Ar-C, *p*-cymene), 67.4 (-$NCH_2$), 42.1 (-$CH_2NH$), 39.9 (N-$CH_2CH_2$, butyl), 30.7 ($CHCH_3$, *p*-cymene), 30.3 (-$CH_2CH_2$, butyl) 23.0 ($CH_3$, *p*-cymene), 21.6 (-$CH_2CH_2$, butyl), 20.4 ($CH_3$, *p*-cymene), 18.9 ($CH_3$, *p*-cymene), 13.9 ($CH_3$, butyl).

*4.4. Synthesis of ($\eta^6$-p-cymene)(N-(2,2'-dipyridylaminoethyl)-1,8-naphthalimide)chloro ruthenium(II) chloride (**8b**).*

The cationic ruthenium(II)-cymene complexes were synthesized using the same procedure as follows [46]. To a solution of [($\eta^6$-cym)$RuCl_2$]$_2$) (0.15 g , 0.30 mmol, 1.0 equiv) in $CH_2Cl_2$ (20 mL) was added N-(2,2'-dipyridylaminoethyl)-1,8-naphthalimide (**8a**) (0.25 g, 0.50 mmol, 2.10 equiv) and stirred at room temperature for 24 h. The solution was filtered through a pad of Celite to remove insoluble materials. The volume of the solution was reduced to ~5 mL and layered with diethyl ether to precipitate the product. The precipitate was isolated *via* filtration, washed with diethyl ether and air dried to give the pure product (**8b**) as an orange solid: (yield: 0.35 g, 80%). Anal. Calcd. for $C_{34}H_{32}N_4O_2Cl_2Ru$: C, 58.29; H, 4.60; 8.00. Found: C, 58.57; H, 4.50; N, 7.52. ESI-MS ($CH_3CN$): m/z = 632.5 [($\eta^6$-*p*-cymene)RuCl(**8a**)–HCl–3H + Li]$^-$. $^1H$ NMR ($CDCl_3$, 400 MHz) δ 8.60 (dd, J = 7.4 Hz, J = 0.9 Hz, 2H, Ar-H), 8.41 (dd, J = 6.0 Hz, J = 1.4 Hz,

2H, Ar-H, Py), 8.22 (dd, J = 8.2 Hz, J = 0.9 Hz, 2H, Ar-H), 8.11 (d, J = 8.2 Hz, 2H, Ar-H), 7.74 (4H, m, Ar-H, Py), 7.0 (t, J= 7.3 Hz, 2H, Ar-H, Py), 5.42 (d, J = 6.4 Hz, 2H, Ar-H, *p*-cymene), 5.27 (d, J = 6.0 Hz, 2H, Ar-H, *p*-cymene), 4.45 (t, J = 5.0 Hz, 2H,-$NCH_2$), 3.97 (t, J = 5.5 Hz, 2H, -$CH_2N$), 2.73 (sept, J = 6.9 Hz, 1H, -$CH(CH_3)_2$, *p*-cymene), 1.94 (s, 3H,$CH_3$, p-cymene), 1.22 (d, J = 6.9 Hz, 6H, $CH(CH_3)_2$, *p*-cymene). $^{13}C$ ($CDCl_3$, 100 MHz) δ 165.0 (C=O), 154.3 (Ar-C, Py), 152.4 (Ar-C), 139.7 (Ar-C), 134.3 (Ar-C), 131.5 (Ar-C, p-cymene), 128.1 (Ar-C), 126.9 (Ar-C), 122.3 (Ar-C), 119.2 (Ar-C), 116.1 (Ar-C), 106.4 (Ar-C), 99.4 (Ar-C, *p*-cymene), 84.4 (Ar-C, *p*-cymene), 61.7 (N-$CH_2$), 42.7 (-$CH_2N$), 30.6 ($CH(CH_3)_2$, *p*-cymene), 22.2 ($CH_3$, *p*-cymene), 18.1 ($CH(CH_3)_2$, *p*-cymene).

*4.5. Synthesis of [($\eta^6$-p-cymene)(N-(2,2'-dipyridylaminepropyl)-1,8-naphthalimide) chlororuthenium(II) chloride* ***(9b)***

The same experimental procedure as reported for **8b**, was used with ligand **9a** to give **9b** as an orange solid (yield: 0.33 g, 77%). Anal. Calcd. for $C_{35}H_{34}N_4O_2Cl_2Ru$: C, 58.82; H, 4.79; N, 7.84. Found: C, 59.15; H, 4.53; N, 7.66. ESI-MS ($CH_3CN$): m/z = 646.7 [($\eta^6$-*p*-cymene)RuCl(**9a**)–HCl–3H + Li]$^-$. $^1H$ NMR ($CDCl_3$, 400 MHz) δ 8.60 (d, J = 7.3 Hz, 2H, Ar-H), 8.41 (d, J = 5.0 Hz, 2H, Ar-H, 2-Py), 8.22 (d, J = 7.8 Hz, 2H, Ar-H), 8.15 (d, J = 7.8 Hz, 2H, Ar-H), 7.76 (m, 4H, Ar-H, Py), 7.03 (t, J = 7.8 Hz, 2H, Ar-H, Py), 5.42 (d, J = 5.0 Hz, 2H, *p*-cymene), 5.27 (d, J = 5.0 Hz, 2H, *p*-cymene), 4.32 (t, J = 6.9 Hz, 2H,-$NCH_2CH_2$), 3.49 (t, J = 6.9 Hz, 2H, -$CH_2CH_2N$), 2.74 (sept, J = 7.0 Hz, 1H, -$CH(CH_3)_2$, *p*-cymene), 2.31 (t, J = 6.9 Hz, 2H, -$CH_2CH_2CH_2$-), 1.95 (s, 3H, $CH_3$, *p*-cymene), 1.23 (d, J = 6.9 Hz, 6H, $CH(CH_3)_2$, *p*-cymene).$^{13}C$ ($CDCl_3$, 100 MHz) δ 164.2 (C=O), 154.3 (Ar-C), 152.4 (Ar-C), 139.7 (Ar-C), 134.1 (Ar-C), 131.5 (Ar-C, *p*-cymene),

131.3 (Ar-C), 128.1 (Ar-C, *p*-cymene), 127.0 (Ar-C), 122.4 (Ar-C), 119.2 (Ar-C), 116.2 (Ar-C), 106.5 (Ar-C), 99.4 (Ar-C), 84.4 (Ar-C, *p*-cymene), 84.3 (Ar-C, *p*-cymene), 39.2 (-$NCH_2CH_2$-), 31.4 (-$CH_2CH_2N$-), 30.7 ($CH(CH_3)_2$), *p*-cymene), 30.5 (-$CH_2CH_2CH_2$-), 22.3 ($CH_3$, *p*-cymene), 18.1 ($CH(CH_3)_2$, *p*-cymene).

**5. Stability Studies**

For stability studies, the UV-vis spectra of 30 μM of the ruthenium(II)-arene complexes (**2b-4b**) and (**8b-9b**) in 1% DMSO at 37 °C in a phosphate buffer saline (PBS) was monitored over 24 h.

**6. DNA Binding Studies**

Concentrated calf thymus DNA (CT-DNA) stock solutions for both absorption and fluorescence studies were prepared in 5 mM Tris-HCl buffer (pH = 7.4) containing 50 mM NaCl. Milli-Q water (18.2 mΩ) was used in all experiments. Concentration of the DNA solution was determined by UV absorbance at 260 nm. The molar absorption coefficient was taken as 6600 $M^{-1}cm^{-1}$. Solutions of CT-DNA gave a ratio of UV absorbance at 260 nm and 280 nm ≥ 1.8, indicating that the DNA solution was sufficiently free of protein. All stock solutions were stored at 4 °C and were used within one week.

*6.1. Absorption titration studies.*

The absorption titrations were performed using fixed concentration of the ligands and the ruthenium(II)-cymene complexes (10 μM), while varying the concentration of CT-DNA from 0-160 μM. After addition of DNA to the ligand and/or metal complex, the resulting solutions were allowed to equilibrate 3-5 min at 25 °C, after which the absorption readings were recorded. The intrinsic binding constants ($K_b$), of the ligands

and the ruthenium(II)-cymene complexes were determined from the spectroscopic titration data using the following equation:$[DNA]/(\varepsilon_a-\varepsilon_f) = [DNA]/(\varepsilon_b-\varepsilon_f) + 1/K_b(\varepsilon_b-\varepsilon_f)$ [47].The 'apparent' extinction coefficient ($\varepsilon_a$) was obtained by calculating $A_{obsd}$/[Ru]. The terms $\varepsilon_f$ and $\varepsilon_b$ correspond to the extinction coefficients of free (unbound) and the fully bound complexes, respectively. The $K_b$ values were calculated from the ratio of the slope to the intercept of a plot of $[DNA]/(\varepsilon_a-\varepsilon_f)$ vs. [DNA] [46].

*6.2. Fluorescence titration studies*

The fluorescence titrations were carried out in 5 mM Tris-HCl buffer (pH = 7.4) containing 50 mM NaCl. Solutions of the ligands and their corresponding metal complexes were titrated with varying concentrations of CT-DNA (0-160 µM). After each addition of CT-DNA, the samples were allowed to equilibrate for 3-5 min prior to recording of the spectra. The data was used to calculate the binding constant ($K_b$) of the ligands and metal complexes.

*6.3. Ethidium Bromide Fluorescence Displacement Experiments*

The ethidium bromide (EB) displacement assay titration experiments were performed on a Varian Cary Eclipse spectrofluorometer using 1 cm path length quartz cell and 5 cm slits. The fluorescence measurements were carried out by successive addition of 0-50 µM of each of the ligands (**2a, 9a**) or the ruthenium complexes (**2b**, **9b**) to a 2.5 mL of a solution that is 40 µM CT-DNA and 5 µM EB in Tris-HCl buffer (pH = 7.4) at room temperature. After each addition of CT-DNA, the solution was stirred for 5 min before measurement. The emission spectra of the EB-DNA system in the presence and absence of solutions of the ligands and ruthenium complexes were

performed by exciting at 520 nm, and the emitted fluorescence was analyzed from 530 to 700 nm at room temperature.

*6.4. Agarose Gel Electrophoresis Experiments*

In the gel electrophoresis experiments supercoiled pUC18 plasmid DNA was treated with freshly prepared solutions (40 μM) of the free ligands (**2a-4a**) and ruthenium complexes (**2b-4b**) in Tris-HCl buffer (5 mM, pH 7.4, 50 mM NaCl) in Milli-Q (18.2 mΩ) water with 5-10% DMSO. The treated DNA samples were incubated at 37 °C for 2 h in the dark. Samples of the treated pUC18 plasmid DNA were loaded on 0.8% (w/v) agarose gel in TAE buffer (Tris-acetate-EDTA buffer, pH = 8.2), and the gel was run for 2.5 h at 70 V. Afterwards, the gel was stained with ethidium bromide (0.5 μg/mL, in TAE) for 5 min, distained in TAE buffer for 15-20 min, and the bands were visualized by photographing the fluorescence of ethidium bromide using a UV illuminator. A sample of pUC18 DNA in TAE buffer alone was used as a control.

**7. Cell Culture and Inhibition of Cell Growth**

*7.1 Cell Culture*

Human melanoma skin cancer cells CRL7687 were obtained from the American Type Culture Collection (ATCC: Manassas, VA) and normal skin melanocytes GM22275 (CA-M75 code in our lab) were obtained from Coriel Cell Repositories (Campton, NJ). The cells were routinely grown in a Dulbecco's Modified Eagle's Medium (DMEM) containing 10% of fetal bovine serum (FBS) at 37 °C with antibiotics in a humidified atmosphere of 5% $CO_2$.

*7.2 Cytotoxicity Assay*

Cytotoxic activity of the compounds was determined using the MTT assay (MTT = 3-(4,5-dimethyl-2-thiazolyl)-2,5-diphenyl-2H-tetrazolium bromide) (Sigma Aldrich C). For evaluation of growth inhibition tests, 1.0 x $10^4$ cells per plate (100 µL) were seeded in 96-well culture plates and grown for 24 h in complete medium prior to addition of the drugs. The stock solutions of the compounds were prepared in DMSO in the concentration ranges of 1.0 x $10^{-2}$ – 2.5 x $10^{-2}$ M. The drug solutions were then directly diluted in the culture medium to concentration ranges of 0-40 µM with a final DMSO concentration of 0.5%, and added to each well. After 72 h incubation at 37 °C, 20 µl of a solution of MTT in PBS (5 mg/mL) was added to each cell, and the plates were incubated for a further 3.5 h at 37 °C. All tests were carried out in triplicate. The culture medium was then aspirated, and the formazan crystals were dissolved in 400 µL of isopropanol in 0.04 M HCl. The absorbance of the plates was read at a 590 nm using microplate reader (Bio-Rad, Hercules, CA, USA) and compared to the values of the control cells incubated without compounds. The $IC_{50}$ values defined as the concentrations of the compounds at which 50% cell growth inhibition is observed were obtained by a Sigma Plot software version 11.0.

## 8. Results and Discussion

*8.1 Synthesis and Characterization*

In the present study, two series of naphthalimide functionalized ligands and their corresponding ruthenium(II)-cymene complexes were synthesized. The first series of ligands **2a-4a** were synthesized *via* the typical condensation route from the reactions of the 5-subtituted-salicylaldehydes with the corresponding 4-[(2'-aminoethyl)amino]-N-

butyl-1,8-naphthalimide precursor (**1)** in refluxing ethanol affording the products as yellow microcrystalline solids in 70-85% yield (Scheme 1).

(Scheme 1 here)

Subsequently, reactions of the dimeric [(*p*-cymene)$RuCl_2]_2$ precursor with two equiv of the N,O-donor ligands **2a-4a** in the presence of potassium *tert*-butoxide (K-$OBu^t$) in dichloromethane gave the neutral half-sandwich mononuclear ruthenimu(II)-cymene complexes (**2b-4b)** as air stable orange or dark red solids in good yield (Scheme 2) [45]. Half-sandwich ruthenium(II)-arene complexes analogous to **2b-4b**, based on similar ligand structural motifs that coordinate to the ruthenium center in an N,O- fashion through the imine nitrogen and the hydroxyl oxygen are known in the literature [45,48-49]. In addition, reported studies by Schmid et al. showed that ligands with similar structures can also coordinate to the ruthenium center in a bidentate N, N-mode through the ethylenediamine moiety [50]. However, these reactions were conducted under base free conditions. In our part, the reactions were conducted in the presence of a base which make the ligands prone to coordinate in an N,O-chelating fashion. All the complexes are soluble in most common organic solvents such as acetone, chloroform, dichloromethane, dimethylformamide (DMF), dimethyl sulfoxide (DMSO) and methanol, but insoluble in water. The N,O-chelating ligands (**2a-4a**) and their corresponding ruthenium(II)-cymene complexes (**2b-4b**) were characterized by means of $^1H$, $^{13}C\{^1H\}$ and electrospray mass spectrometry (ESI-MS).

(Scheme 2 here)

The $^{1}$H NMR spectra of the ligands **2a-4a** show characteristic peaks corresponding to the imine (N=CH) linkage between 8.31-8.65 ppm. The signals for the methylene protons of the aminoethyl moiety also appeared at 3.77-4.00 ppm. The naphthalimide and phenyl ring resonances appear between 6.67-8.61 ppm. The remaining signals in the $^{1}$H NMR spectra of the ligands **2a-4a** show the expected resonances for the aliphatic protons (see experimental part). Similarly, the $^{13}$C{$^{1}$H} spectra of the ligands **2a-4a** also display characteristic peaks between 166.0-167.2 ppm assigned for the carbonyl carbons and peaks at 164.4-165.8 ppm corresponding for the imine carbon. The structures of the ligands **2a-4a** were further confirmed by ESI-MS. Acquired in the positive ion mode, acetonitrile solutions of the N,O-chelating ligands (**2a-4a**) show strong peaks corresponding to the molecular ions as [**2a** + H]$^{+}$ for (**2a**); [**3a**]$^{+}$ and [**4a**]$^{+}$ for **3a** and **4a**.

The NMR and ESI-MS spectral data strongly support the proposed structures of the neutral half sandwich ruthenium(II)-cymene complexes. This reaction also results in the formation of chiral complexes with the ruthenium center being the stereogenic center and the ligands acting as bidentate N,O-chelates. Hence, in the $^{1}$H NMR spectra the complexes **2b-4b** display four separate doublets for the aromatic protons of the *p*-cymene (5.00-5.59 ppm) and two doublets each for the methyl protons (1.17-1.26 ppm) of the isopropyl group. The nonequivalence of the protons in both the aromatic ring and the isopropyl group indicate the absence of any symmetry element in the complexes, reflecting the asymmetric coordination of the chelating N,O-donor ligands to the ruthenium center. The coordination of the $\eta^{6}$-cymene ring to the ruthenium(II) center is also clearly indicated by the $^{1}$H NMR spectra, in which the resonances of the aromatic

protons (5-5.63 ppm) are considerably upfield shifted compared to those of the free arene. The septet corresponding to the isopropyl proton was observed near the 2.74-2.76 ppm, and the singlet for the methyl protons at 2.30-2.33 ppm. Apart from these signals, the $^{1}$H NMR spectra of **2b-4b** display resonances at 7.07-7.31 ppm corresponding to the imine HC=N proton, which are significantly upfield shifted compared to those of the free ligands (8.31-8.65 ppm), suggesting coordination of the imine nitrogen to the ruthenium(II) ion. However, signals attributed to the protons of the 1,8-naphthaimide moiety do not show a noticeable shift upon coordination of the ligands to the ruthenium(II) center, indicating that the naphthalimide does not significantly interact with the ruthenium center. In addition, in the $^{13}$C{$^{1}$H} NMR spectra of the complexes, six well separated resonances were observed for the aromatic carbons of the *p*-cymene moiety (see experimental part). The imine carbons (HC=N) exhibit peaks in the region 164.2-166.5 ppm. The remaining $^{1}$H and $^{13}$C{$^{1}$H} signals show chemical shifts typical of the aliphatic region along with signals in the aromatic region due to both the 1,8-naphthalimide and phenyl ring. Any attempts to obtain crystals of **2b-4b** suitable for X-ray structural analysis were unsuccessful.

Electrospray ionization mass spectra (ESI-MS) provided further evidence for the formation of the ruthenium(II)-cymene complexes. The mass spectra of acetonitrile solutions of the complexes **2b-4b** show peaks corresponding to the [[($\eta^6$-*p*-cymene)RuCl(**2a-4a**)–Cl]$^{+}$ ion for **2b**, **3b** and **4b**, respectively corroborating their structures.

The second groups of ligands **8a-9a** were also easily prepared in good yield by reacting the naphthatlimide functionalized intermediate compounds (**7**) with 2,2'-

dipyridylamine in the presence of a slight excess of $Cs_2CO_3$ in acetonitrile at room temperature (Scheme 3) [44].

(Scheme 3 here)

The synthesis of the cationic mononuclear ruthenium(II)-cymene complexes **8b** and **9b** was achieved via the bridge cleavage of the $[(\eta^6\text{-}p\text{-cymene})RuCl_2]_2$, dimer with 2.1 equiv of the 1,8-naphthalimide–tethered 2,2'-dipyridylamine ligands (**8a, 9a**) in $CH_2Cl_2$ at room temperature for 24 h in 77-80% yield (Scheme 4) [46]. Isolated as their chloride salts, complexes **8b** and **9b** are air-stable red-orange solids, that dissolve in most common organic solvents (acetone, acetonitrile, dichloromethane, DMSO, DMF and methanol) and slightly soluble in water. The ligands and the new ruthenium(II)-cymene complexes were characterized by $^1H$, $^{13}C\{^1H\}$ NMR and ESI-MS spectroscopy.

(Scheme 4 here)

The $^1H$ NMR spectrum of **8a** displays two well-separated triplet resonances at 3.99 and 4.46 ppm attributed to the methylene protons. The CH protons adjacent to the nitrogen atom of the 2,2'-dipyridylamine unit also display doublet resonances at 8.26 ppm. The remaining $^1H$ and $^{13}C$ NMR spectra show all the expected resonances for the 1,8-naphthalimide and 2.2'-dipyridyl amine moieties. The main NMR spectroscopic properties of **9a** are similar to those of **8a**. The ESI-MS spectra of acetonitrile solutions of the ligands **8a** and **9a** show peaks corresponding to the $[\mathbf{8a} + H]^+$ and $[\mathbf{9a}]^+$ ions.

Both the $^1H$ and $^{13}C\{^1H\}$NMR spectra confirm coordination of the ligands **8a** and **9a** to the ruthenium center. The $^1H$ NMR spectra of the ruthenium(II)-cymene complexes **8b** and **9b** contain resonances at ca. 8.41 ppm attributed to the C**H** groups (2H) adjacent to the pyridine nitrogen, indicating the symmetrical coordination of the N,N-chelating

ligands to the ruthenium by the pyridine nitrogen atoms. These resonances are shifted downfield relative to the free ligands from 8.26 ppm to 8.41 ppm indicating coordination of the ruthenium(II) ion to the nitrogen atoms of the 2,2'-bipyridylamine ligands. In addition to this the symmetrical nature of the compounds was evidenced by the observation of two sets of doublets for the aromatic protons on the *p*-cymene ligand (5.27- 5.43 ppm). The $^{1}$H NMR spectra of the complexes (**8b, 9b**) also exhibit sets of doublet peaks for the methyl protons of the isopropyl group. Likewise, a septet at ca. 2.60-2.80 ppm is observed for the isopropyl proton. The $^{13}C\{^{1}H\}$ NMR spectrum also exhibits appropriate signals. The methyl carbons display signals in the range 15 and 30 ppm. The methyl carbons of the isopropyl group appear around 29-34 ppm, while the cymene carbons appear in the range 84.35-99.44 ppm for the C-H carbons. These chemical shifts are similar to those reported for similar ruthenium arene compounds [44]. The carbons of the 1,8-naphthalimide and 2,2'-dipyridylamine groups give peaks in the range 116-165 ppm. The remaining $^{1}$H and $^{13}C\{^{1}H\}$ signals show chemical shifts typical of the aliphatic region along with signals in the aromatic region due to both the 1,8-naphthalimide and pyridine moieties.

Electrospray ionization mass spectrometry (ESI-MS) provided further evidence for the formation of the ruthenium(II)-cymene complexes. The ESI-MS of the complexes **8b** and **9b** measured in the negative ion mode in acetonitrile showed peaks corresponding to the fragment ions $[[(\eta^6\text{-}p\text{-cymene})RuCl(\mathbf{8a})–HCl–3H + Li]^-$ for **8b** and $[[(\eta^6\text{-}p\text{-cymene})RuCl(\mathbf{9a})–HCl–3H + Li]^-$ for **9b**.

**9. Stability Studies**

The stability of the ruthenium(II)-arene complexes (**2b-4b**) and (**8b-9b**) was studied at 37 °C in PBS containing 1% DMSO over 24 h by UV-vis absorption spectroscopy. As representative examples, the UV-vis spectral profiles of complexes **2b** and **9b** are shown in Figure 1. The absorption spectra of **9b** remains quite stable with no

Figure 1 here

significant shift in the $\lambda_{max}$ (345 nm) value in the aqueous buffer solution with 1% DMSO (Fig.1b). Complex **8b** also exhibits similar spectral profile as shown in Figure S1b. In contrast, the UV-vis spectra of complex **2b** display significant decrease in the maximum absorbance at 440 nm in PBS (Fig.1a). Likewise, complexes **3b-4b** show very similar UV-vis absorption profiles to that of **2b** (Fig. S1a and S2). On the other hand, as is also found for complexes **8b-9b**, no significant shift in the $\lambda_{max}$ values was observed for **2b-4b**. However, a slight cloudiness was observed in the aqueous and 1% DMSO solutions of complexes **2b-4b** after 24 h at 37 °C. Hence, the decrease in absorbance of complexes **2b-4b** is probably due to the partial dissociation of the ruthenium(II) complexes, which results in lowering of their concentrations in solution. Overall, the results of the UV-vis studies indicate that the ruthenium(II) complexes **8b-9b** are quite stable in the aqueous PBS solution, while the complexes **2b-4b** undergo hydrolysis to a certain extent. However, despite the difference in stability of the complexes, there does not appear to be a strong correlation between hydrolysis and cytotoxicity, both series of complexes (**2b-4b**) and (**8b-9b**) essentially displaying similar cytotoxic profiles (Table 1).

## 10. Biological Evaluations

*10.1. In vitro cytotoxic activity*

The *in vitro* cytotoxicity of the 1,8-naphthalimide-tagged free ligands (**2a** and **9a**), and the ruthenium(II)-cymene complexes (**2b-4b** and **8b-9b**) were evaluated against the human melanoma skin cancer cell line (CR7687) by means of the colorimetric MTT assay. The results obtained from the UV-vis titration studies indicated that the ligands; **2a-4a**, with bromo, chloro and nitro substituents at the para position of the phenyl ring, respectively, bind to CT-DNA in a similar fashion (*vide infra*). Similarly, the second series of ligands; **8a-9a,** containing two different aliphatic linkers also showed comparable binding ability to CT-DNA. Due to these similarities, the ligands **2a** and **9a** were selected as representative members of the ligand systems explored in this study to evaluate their *in vitro* cytotoxicity. The inhibitory percentage against growth of cancer cells was determined after treatment of the cells with different concentrations of the free ligands and the metal complexes for 72 h. In addition, in order to evaluate the selectivity of the compounds for cancerous cells rather than healthy cells, the compounds were also tested for their cytotoxic activity against the normal skin melanocytes (CA-M75). The $IC_{50}$ values of both the free ligands and their corresponding ruthenium(II)-cymene complexes are summarized in Table 1.

(Table 1 here)

The following general conclusions can be drawn based on the results displayed in Table 1: First, it is evident that both the naphthalimide based representative ligands (**2a** and **9a**), and the new ruthenium(II)-cymene complexes (**2b-4b**, and **8b-9b**) exhibit significant cytotoxic activities against the melanoma cell line tested, with $IC_{50}$ values in

the submicromolar ranges (0.62-1.10 μM). In addition, in the first series of complexes, the nature of substituent groups, chloro (**2b**), bromo (**3b**) and nitro (**4b**) in the *para* position of the phenyl ring have no significant influence on the *in vitro* antitumor activity; to within experimental errors, all the complexes showing almost the same cytotoxicity. Likewise, in the second series of compounds **8b** and **9b**, the spacer length between the naphthalimide moiety and 2,2'-dipyridylamine unit has minor influence on the cyctotoxic activity of the complexes. Compound **8b** with the ethyl linker exhibited slightly higher anticancer activity compared to that of the ruthenium(II) compound with the propyl linker, **9b**. Second, in the first series of compounds both the free ligands and their corresponding ruthenium(II)-cymene complexes showed comparable cytotoxicities towards the human melanoma skin cancer cell line tested. This indicates that conjugation of the ruthenium(II)-cymene fragment with the naphthalimide functionalized ligands provides no additional advantages in improving the cytotoxicity of the complexes. Naphthalimide and its derivatives are known bioactive molecules with potent cytotoxic activities. In fact, two of its derivatives have been widely investigated and entered into clinical trials as potential anticancer drugs [32-34]. Hence, the bioactive naphthalimide moiety is probably mainly responsible for the antiproliferative activity of these new ruthenium(II)-cymene complexes.

Furthermore, it is notable that the free ligand **2a** and the ruthenium(II)-cymene complexes (**2b-4b**) display similar cytotoxicities towards the cancerous and normal cells, which indicates that these compounds are not selective. In contrast, in the second series of compounds (**8b-9b**), coordination of the naphthalimide-functionalized N, N-chelating ligands to the ruthenium(II)-cymene unit leads to a significant increase in selectivity of

the complexes for tumors rather than the normal cells. For example, the free ligand **9a** has an $IC_{50}$ value of 0.620 μM against the melanoma skin cancer cell line (CR7686) and an $IC_{50}$ value of 0.613 μM against the normal skin melanocytes (CA-M75). In comparison, complex **9b** displays more toxicity towards the cancerous cells ($IC_{50}$ of 1.103 μM), which much lower than that for the normal cells ($IC_{50}$ of 19.70 μM).

The reason for the selectivity of complex **9b** needs further investigation which is currently undergoing in our lab. However, some preliminary assessments can be drawn that correlate the selectivity of the compound; **9b** to the spacer length between the naphthalimide and the N,N-chelating ligands in the complex. The longer the alkyl chain the more selective the compound. Thus, it may be likely that the presence of the cationic charge and the longer propyl linker are influencing the biological activities and the selectivity of the complex **9b**.

**10.2 DNA-Binding Studies**

While the exact mode of action of the cytotoxic ruthenium(II)-arene complexes is not clearly understood yet, DNA is considered to be one of their potential biological targets [51-55]. Hence, to evaluate the mode of interactions of the new ruthenium(II)-cymene complexes explored in the present study with DNA, UV-vis absorption and fluorescence spectroscopy, and gels electrophoresis studies were carried out.

*10.2.1 Electronic absorption titration studies*

Electronic absorption titration studies of the ligands **2a-4a**, along with their metal complexes **2b-4b** were carried out to evaluate their DNA binding properties. The absorption spectra of the ligands show intense bands at $\lambda_{max}$ 440 nm (**2a**), 437 nm (**3a**), and 408 nm (**4a**). Similarly, the corresponding metal complexes display intense bands at

$\lambda_{max}$ 444 nm (**2b**), 442 nm (**3b**), and 412 nm (**4b**) with a slight red shift (1-2 nm) compared to those of the free ligands. The ligand **4a** and its ruthenium(II) complex **4b** which have a nitro substituent at the 5-postion of the phenyl ring have an absorption maximum slightly lower (408 nm for **4a**) and (412 nm for **4b**) compared to those of the chloro- and bromo substituents. The difference in the maximum absorption peaks could mainly be due to the strong electron withdrawing capacity of the nitro-substituent on the phenyl ring. Otherwise, all the ruthenium(II)-cymene complexes have photophysical properties similar to those observed in the free ligands, indicating that these bands are mainly due to the 1,8-naphthalimide chromophore. Since the ligands and their metal complexes have similar structural features, and displayed comparable cytotoxic activities, the ligand **2a** and its metal complex **2b** are selected for discussions of their DNA binding as typical examples.

The electronic absorption titration data for **2a** and **2b** in the absence and presence of CT-DNA are given in Figures 2 and 3. Addition of increasing amounts of CT-DNA (0-160 μM) to constant concentrations (10 μM) of **2a** and/or **2b** resulted in a significant reduction in the absorption spectra along with a slight red shift (1-2 nm). For **2a** the absorption spectra at $\lambda_{max}$ 440 nm exhibited 28% hypochromism upon binding to CT-DNA. Likewise, significant changes were also observed for the metal complex **2b**, where the absorption spectra showed 30% hypochromism at $\lambda_{max}$ 444 nm upon binding to CT-DNA. In general, significant hypochromism and large red shifts of the absorption spectral bands are characteristics of compounds that interact with DNA by a strong intercalative mode [56-59]. The observed hypochromism in the spectra of CT-DNA upon addition of **2a** and/or **2b** can be partially evidenced as binding *via* intercalation through the

naphthalimide part; as DNA intercalators, in general, leads to a hypochromic effect [29, 36]. However, the observed low hypochromism with no red shift in the band position could also suggest an electrostatic mode of DNA binding of the ligands and the new metal complexes. Overall, the results suggested that the ligands and the new metal complexes interact with CT-DNA, but the extent of interaction is weak. These characteristic spectral changes are also very similar to those reported in the literature that involves weak naphthalimide-DNA interactions [36].

((Figure 2 here)

(Figure 3 here)

The intrinsic binding constant $K_b$ of the compounds **2a** and **2b** was also determined by monitoring the changes in absorbance at the corresponding maximum wavelengths. Obtained as the ratio of the slope to intercept from the plot of [DNA]/($\varepsilon_a$-$\varepsilon_f$) versus [DNA], the values of the binding constant showed that **2b** have high DNA binding propensity $K_b = 2.0 \times 10^4\ M^{-1}$, while **2a** gave $K_b = 5.0 \times 10^3\ M^{-1}$, which is in agreement with the observed hypochromism trends. The higher DNA binding affinity of the ruthenium complex **2b** relative to the corresponding free ligand **2a** may suggest that the 1,8-naphthalimide pharmacophore and the ruthenium(II) ion may be interacting in a cooperative manner through intercalation and covalent coordination. Similar binding constant values were obtained for the ligands **3a-4a** and the ruthenium(II) complexes **3b-4b**. The absorption spectra of the compounds (**3a and 3b**) and complexes (**4a and 4b**) are given as supporting materials in Figures S3-S4.

The DNA binding properties of the ligand **8a** and its ruthenium complexes **8b** were also investigated in a manner similar to those of **2a** and **2b** described above. The

absorption spectra of **8a** and **8b** in Tris-HCl buffer (5 mM, pH = 7.4, 50 mM NaCl) are shown in the supporting information (Fig. S5a-S6a). The titration was performed by adding increasing amounts of CT-DNA (0-160 μM) to constant concentrations (20 μM) of **8a** and (50 μM) of **8b,** respectively.

Upon addition of CT-DNA, the absorption band centered at 304 nm for **8a** was significantly decreased showing ca 41% hypochromism with no shift in the absorption maximum. Likewise, the ruthenium complex **8b** exhibited similar changes, where the absorption spectra showed ca. 46% hypochromism at $\lambda_{max}$ 337 nm upon addition of increasing amounts of CT-DNA. The binding constant values of the ligand and its ruthenium complex were also obtained and found to be $K_b = 1.0 \times 10^4\ M^{-1}$ for **8a** and $K_b = 6.0 \times 10^4\ M^{-1}$ for **8b**. Similar values were also obtained for **9a** and **9b** (Fig. S7a – S7b). As molecules that contain the 1,8-naphthalimide structure have been known to be strong DNA intercalating agents, the new ligands and their metal complexes were expected to interact with DNA [30-32].

*10.2.2 Fluorescence titration studies*

To further investigate the DNA-binding properties of the ligands and their ruthenium complexes, fluorescence spectral studies were also carried out in Tris-HCl buffer (5 mM, pH 7.4, 50 mM NaCl). The fluorescence emission band of **2a** ($\lambda_{ex}$ = 435 nm) is obtained at 532 nm (Fig. 4), and upon addition of increasing concentrations of CT-DNA significant quenching in the fluorescence intensity of the 532 nm band with a slight red shift could be observed. Likewise, the metal complex **2b** shows a fluorescence emission band at 538 nm ($\lambda_{ex}$ = 480 nm). Upon addition of increasing amounts of CT-

DNA to the solution of **2b**, a clear quenching of the fluorescence emission ($\lambda_{max}$ = 538 nm) along with slight red shift (Fig. 5) was observed. The quenching of the emission intensity may be attributed to an efficient photoinduced electron transfer (PET) from the DNA bases to the excited states of the 1,8-naphthalimide pharmacophore [36]. The binding constant values obtained from the emission titrations experiments are $K_b$ = 5.0 x $10^2$ $M^{-1}$ for **2a** and $K_b$ = 2.0 x $10^3$ $M^{-1}$ for **2b**. Such fluorescence quenching in the presence of DNA is common in metal complexes containing intercalating agents and has been described in the literature [56-59]. The modest hypochromism in the fluorescence intensity suggests that the new ligands and the metal complexes are interacting with DNA moderately.

(Figure 4 here)

(Figure 5 here)

The emission properties of the ligand **8a** and its ruthenium complex **8b** were also studied. As shown in Figure S5b and S6b in the supporting materials, the fluorescence spectra of **8a** and **8b** show an emission band at 396 nm, and upon addition of increasing amounts of CT-DNA the fluorescence intensity slightly decreases without any significant change in the emission maxima. The binding constants obtained from the fluorescence titration experiments were found to be 1.0 x $10^2$ $M^{-1}$ and 1.6 x $10^3$ $M^{-1}$ for **8a** and **8b**, respectively.

In general, the results obtained from the UV-vis absorption and fluorescence titration studies suggest that the new ligands and their corresponding ruthenium complexes can bind with CT-DNA presumably through intercalative binding mode. The slight difference in binding constants obtained between the UV-vis and fluorescence

methods may be arising from the use of two different plotting methods. However, the results obtained from the above absorption and fluorescence titration studies indicate the presence of moderate interaction between DNA and the ligands and their corresponding metal complexes.

*10.2.3 Ethidium bromide-DNA (EB-DNA) quenching assay*

To further evaluate other possible DNA binding modes of the ligands and their metal complexes, the ethidium bromide (EB) displacement assay was carried out in 5 mM Tri-HCl buffer (pH 7.4). As a classical intercalator, EB emits an intense fluorescence in the presence of DNA. The quenching of the emission intensities of the maximum wavelength of the EB bound to DNA are interpreted as the displacement of EB from the EB-DNA system, and the intercalative binding of the compound to DNA. In this study, the competitive bindings of **2a** and **2b** to CT-DNA were measured by monitoring the changes in the emission spectra of EB bound to DNA upon successive addition of 0-50 µM aliquots of either **2a** or **2b**. As shown in Figures 6 and 7, titration of the solution of DNA pretreated with EB with the ligand **2a** and/or the ruthenium complex **2b** resulted in a reduction in the emission intensity of EB bound to CT-DNA. Compared to the initial intensity, addition of increasing amounts of **2a** or **2b** leads to significant hypochromism with no red shift. This suggests that the EB molecules bound to DNA are displaced by the compounds investigated in this study [60]. The titration data also allowed for the determination of the quenching constant of the ligands and metal complexes to CT-DNA by calculating the Stern-Volmer quenching constant using the equation: $F_0/F = 1 + K_{sv}[Q]$. $F_0$ and F are the fluorescence intensity of the CT-DNA solution in the absence and presence of the compounds, $K_{sv}$ is the Stern-Volmer quenching constant and [Q] is

concentration of the ligand **2a** or the ruthenium complex **2b**. Obtained as slope from the plots of $F_o/F$ *vs.* [Q], which are shown as an inset in Figures 5 and 6, the $K_{sv}$ values were found to be 5.2 x $10^3$ and 1.1 x $10^4$ $M^{-1}$ for **2a** and **2b**, respectively.

(Figure 6 here)

(Figure 7 here)

The $K_{sv}$ value of the metal complex **2b** is higher than that of the free ligand **2a**, which is in agreement with the results obtained from the electronic absorption spectra. In addition, the values of the quenching constant indicate that both compounds are capable of displacing EB form the EB/CT-DNA system. The good linear fit of the Stern-Volmer plots also indicate the existence of only one kind of quenching process. Furthermore, the titration measurements were used to determine the apparent DNA binding constant ($K_{app}$) of the ligand **2a** and its metal complex **2b** using the equation: $K_{EB}[EB] = K_{app}[Q]$ where [Q] is the concentration of **2a** or **2b** at the 50% reduction in the fluorescence intensity of EB, $K_{EB}$ (1.2 x $10^7$ $M^{-1}$) is the DNA binding constant of EB, and [EB] is the concentration of EB (5 μM). The $K_{app}$ values were found to be 8.9 x $10^5$ and 5.0 x $10^5$ for **2a** and **2b**, respectively. The results of the observed quenching constants and the apparent binding constants of the free ligand **2a** and the ruthenium complex **2b** suggest that both compounds are capable of interacting with DNA in an intercalative binding mode. Similarly, the values of the quenching constants, $K_{sv}$, for **8a** and **8b** were determined and found to be 4.6 x $10^3$ $M^{-1}$ and 6.6 x $10^3$ $M^{-1}$, respectively (Fig. S8a and S8b).

*10.2.4 Gel electrophoresis assay*

The interaction of **2a-4a** and **2b-4b** with DNA was also further studied by testing the ability of the compounds to alter the electrophoretic mobility of supercoiled pUC18 plasmid DNA. A representative gel of pUC18 plasmid DNA treated with 40 μM solutions of **2a-4a** and **2b-4b** in the dark at 37 ºC for 2 h is shown in Figure 8.

(Figure 8 here)

The results showed that the ligands and the ruthenium(II) complexes did not significantly change the supercoiled DNA or the relaxed form, as indicated by the migration rate and proportions. This indicated that both the ligands and the new metal complexes have weak unwinding ability for supercoiled DNA. However, a slightly higher conversion of the supercoiled DNA into the relaxed form was observed in the presence of complex **3b** (lane 6) compared to the free ligands **2a-4a** (lanes 2-4) and the other metal complexes **2b** and **4b** (lanes 3, 5, 7).

**11. Conclusions**

Two new series of mononuclear ($\eta^6$-*p*-cymene)Ru(II) complexes bearing naphthalimide conjugated chelating ligands have been synthesized and characterized by a variety of spectroscopic methods. The *in vitro* cytotoxic activity of the compounds has been evaluated against the CRL8678 human melanoma skin cancer and CA-M75 noncancerous cell lines. The new naphthalimide conjugated compounds exhibit significant antiproliferative activities, with $IC_{50}$ values in the low μM ranges. However, in both series of compounds binding of the biologically active naphthalimide moiety to the ruthenium(II)-arene unit didn't afford complexes with more potent cytotoxic

activities, with ligands and their corresponding metal complexes displaying nearly the same cytotoxicities. Variations of the substituent groups in the *para* position of the phenyl ring of the N,O- based chelating ligands have no significant effect on cytotoxicity. However, the ruthenium(II)-arene complexes derived from the N,N-based chelating ligands displayed good selectivity toward cancer cells over the normal CA-M75 cells, and the selectivity increases with decrease in the linker chain length. Furthermore, the UV-Vis and fluorescence spectra, and gel electrophoresis studies suggest that the new compounds interact with DNA mainly via intercalation mode of the naphthalimide group.

**Acknowledgments:** We wish to thank the National Science Foundation CREST center (HRD-1137747) and the Hampton University Faculty Research Fund for financial support. Dr. Anand Iyer (College of Pharmacy, Hampton University) is thanked for assistance in the calculation of the $IC_{50}$ values. The authors also thank Dr. Ei Ei Brown (Department of Physics, Hampton University) for helping with the fluorescence measurements.

**Authors Contributions:**

All authors agree on the final version of the manuscript

Contribution of individual authors to the experimental work and manuscript are as follows:

**Ashley Peralta** (undergraduate student) and **Dr. Kesete Ghebreyessus** were involved in the synthesis and characterization of the compounds, and analysis of the DNA-binding studies using UV-vis absorption and fluorescence spectroscopy.

**Dr. Shanthi Paranawithana** was involved in the gel electrophoresis studies and analysis.

**Dr. Meena Katdare** and Krishnan Prabhakaran from the Skin of Color Cancer research Institute were involved in the cell culture and cytotoxicity assay experimental work and analysis.

**Conflict of Interest Disclosure:**

The authors declare no competing financial interest

## 12. References

[1] C. G. Hartinger, P. J. Dyson, *Chem. Soc. Rev. 38* (2009) 391-401.
[2] S. H. van Rijt, P. J. Sadler, *Drug Discovery Today* 14 (2009) 1089-1097.
[3] M. J. Clark, *Coord. Chem. Rev.* 236 (2003) 209-233
[4] M. A. Jakupec, M. Galanski, V. B. Arion, C. G. Hartinger, B. K. Keppler, *Dalton* S. P. Fricker, *Dalton, Trans.* (2007) 4903-4917.
[5] Z. Guo, P. J. Sadler, *Adv. Inorg. Chem.* 49 (2000), 183-306.
[6] C. G. Hartinger, M. A. Jakupec, S. Zorba-Seifried, M. Groessl, A. Egger, W. Berger, H. Zorbas, P. J. Dyson, B. K. Keppler, *Chem. Biodiversity* 5 (2008) 2140-2155.
[7] J. M. Rademaker-Lakhai, D. Van den Bongard, D. Pluim, J. H. Beijnen, J. H. M. Schellens, *Clin. Cancer Res.* 10 (2004) 3717-3727.
[8] C. G. Hartinger, M. A. Jakupec, S. Zorba-Seifried, B. Kynast, H. Zorbas, B. K. Keppler, *J. Inorg. Biochem.* 100 (2006) 891-904.
[9] E. Alessio, G. Mestroni, A. Bergamo, G. Sava, *Curr. Top. Med. Chem.* 4 (2004) 1525-1535.
[10] P. J. Dyson, G. Sava, *Dalton Trans.* (2006) 1929-1933.
[11] P.-S. Kuhn, V. Pichler, A. Roller, M. Hejl, M. A. Jakupec, W. Kandioller, B. K. Keppler, *Dalton Trans.* (2015) 659-668.
[12] R. Trondl, P. Heffeter, C. R. Kowol, M. A. Jakupec, W. Berger, B. K. Keppler, *Chem. Sci.* 5 (2014) 2925-2932.
[13] M. Groessl, E. Reisner, C. G. Hartinger, R. Eichinger, O. Semenova, A. R. Timerbaev, M. A., Jakupec, V. B. Aaron, B. K. Keppler, *J. Med. Chem.* 50 (2007) 2185-2193.
[14] A. M. Pizarro, P. J. Sadler, *Biochimie* 91 (2009) 1198-1211.
[15] J. Reedijk, *Platinum Met. Rev.* 52 (2008) 2-11.
[16] R. E. Morris, R. E. Aird, M. D. S. Piedad, H. Chen, J. Cummings, N. D. Hughes, S. Parsons, A. Parkin, G. Boyd, D. I. Jodrell, P. J. Sadler, *J. Med. Chem.* 44 (2001) 3616-3621.
[17] H. Chen, J. A. Parkinson, R. E. Morris, P. J. Sadler, *J. Am. Chem. Soc.* 125 (2003) 173-186.
[18] S. H. van Rijt, A. J. Hebden, T. Amaresekera, R. J. Deeth, G. J. Clarkson, S.

Parsons, P. C. McGowan, P. J. Sadler, *J. Med. Chem.* 52 (2009) 7753-7761.
[19] P. C. Bruinjnincx, P. J. Sadler, *Curr. Op. Chem. Biol*. 12 (2008) 197-206.
[20] R. Fernandez, M. Melchart, A. Habtemariam, S. Parsons, P. J. Sadler, *Chem-Eur. J.* 10 (2004) 5173-5179.
[21] A. Habtemariam, M. Melchart, R. Fernandez, S. Parsons, I. D. H. Oswald, A. Parkin, F. P. A. Fabbiani, J. E. Davidson, R. E. Aird, D. I. Jodrell, P. J. Sadler, *J. Med. Chem.* 49 (2006) 6858-6868.
[22] S. Chatterjee, S. Kundu, A. Bhattacharyya, C. G. Hartinger, P. J. Dyson, *J. Biol. Inorg. Chem.* 13 (2008) 1149-1155.
[23] C. Scolaro, A. Bergamo, L. Brescacin, R. Delfino, M. Cocchietto, G. Laurenczy, T. J. Geldbach, G. Sava, P. J. Dyson, *J. Med. Chem.* 48 (2005) 4161-4171.
[24] C. Scolaro, T. J. Geldbach, S. Rochat, A. Dorcier, C. Gossens, A. Bergamo, M. Cocchietto, I. Tavernelli, G. Sava, U. Rothlisberger, P. J. Dyson, *Organometallics* 25 (2006) 756-765.
[25] W. H. Ang, E. Daldini, C. Scolaro, R. Scopellitti, L. Juillerat-Jeanneret, P. J. Dyson, *Inorg. Chem.* 45 (2006) 9006-9013.
[26] E. A. Hilliard, A. Vessières, G. Jaouen, *Top. Organomet. Chem.* 32 (2010) 81-117.
[27] W. H. Ang, L. J. Parker, A. De Luca, L. Juillerat-Jeanneret, C. J. Morton, M. Lo Bello, M. W. Parker, P. J. Dyson, *Angew. Chem., Int. Ed.* 48 (2009) 3854-3857.
[28] Jaouen, G., Ed.; "Bioorganometallics:" Wiley-VCH, Germany, 2006 p 444.
[29] K. J. Kilpin, C. M. Clavel, F. Edafe, P. J. Dyson, Organometallics 31 (2012) 7031-7039.
[30] L. Xie, Y. Xu, F. Wang, J. Liu, X. Qian, J. Cui, *Bioorg. Med. Chem.*17 (2009) 804-810.
[31] L. Ingrassia, F. Lefranc, R. Kiss, T. Mijatovic, *Curr. Med. Chem.* 16 (2009) 1192-1213.
[32] C. Bailly, *Chem. Rev.* 112 (2012) 3611-3640.
[33] M. F. Brana, J. M. Castellano, M. Moran, M. J. Perez de Verga, C. R. Romerdahl, D. X. Qian, P. Bousquet, F. Emling, E. Schlick, G. Keilhauer, *Anti-Cancer Drug Des.* 8 (1993) 257-264.
[34] Z. Chen, X. Liang, H. Zhang, H. Xie, J. Liu, Y. Xu, W. Zhu, Y. Wang, X. Wang, S. Tan, D. Kuang, X. Qian, *J. Med. Chem.* 53 (2010) 2589-2595.
[35] W. W. Cholody, T. Kosakowsaka-Cholody, M. G. Hollingshead, H. K. Hariprakasha, C. J. Michejda, *J. Med. Chem.* 48 (2005) 4474-4481.
[36] E. B. Veal, T. Gunnlaugsson, *J. Org. Chem.* 75 (2010) 5513-5525.
[37] I. Ott, Y. Xu, J. Liu, M. Kokaschka, M. Harlos, W. S. Sheldrick, X. Qian, *Bioorg. Med. Chem.* 16 (2008) 7107-7116.
[38] D. W. Cho, M. Fujitsuka, K. H. Choi, M. J. Park, U. C. Yoon, T. Majima, *J. Phys. Chem. B* 110 (2006) 4576-4583.
[39] G. J. Ryan, S. Quinn, T. Gunnlaugsson, *Inorg. Chem.* 47 (2008) 401-403.
[40] B. A. Teicher, M. J. Abrams, K. W. Rosbe, *Cancer Res.* 50 (1990) 6971-6975.
[41] M. A. Bennet, A. K. Smith, *Dalton Trans.* (1974) 233-242.
[42] X. Zeng, X. Zhang, B. Zhu, H. Zia, Y. Li, *Dyes and Pigments* 94 (2012) 10-15.
[43] N. I. Georgiev, V. B. Bojinov P. S. Nikolov, *Dyes Pigments* 81 (2009) 18-26.
[44] S. Y. Kim, J.-I. Hong, *Tetrahedron Lett.* 50 (2009) 2822-2824.
[45] H. Brunner, T. Zwack, M. Zabel, W. Beck, A. Böhm, *Organometallics* 22 (2003)

1741-1750.
[46] P. Haquette, B. Dumat, B. Talbi, S. Arbabi, J.-L. Renaud, G. Jaouen, M. Salmain, *J. Organomet. Chem.* 694 (2009) 937-941.
[47] A. Wolfe, G. H. Shimer, T. Meehan, *Biochemistry* 26 (1987) 6392-6401.
[48] L. Glans, A. Ehnbom, C. de Kock, A. Martínez, J. Estrada, P. J. Smith, M. Haukka, R. A. Sanchez-Delgado, E. Nordlander, *Dalton Trans.* 41 (2012) 2764-2773.
[49] P. Govender, A. K. Renfrew, C. M. Clavel, P. J. Dyson, B. Therrien, G. S. Smith, *Dalton Trans.* 40 (2011) 1158-1167.
[50] W. F. Schmid, R. O. John, V. B. Arion, M. A. Jakupec, B. K. Keppler, *Organomettalics,* 26 (2007) 6643-6652.
[51] O. Novakova, H. Chen, O. Vrana, A. Rodger, P. J. Sadler, V. Brabec, *Biochemistry,* 42 (2003)11544-1155.
[52] T. Bugarcic, O. Novakova, A. Halamikova, L. Zerzankova, O. Vrana, J. Kasparova, *J. Med. Chem.* 51 (2008) 5310-5319.
[53] H. Chen, J. A. Parkinson, R. E. Morris, P. J. Sadler, *J. Am. Chem. Soc.* 125 (2003) 173-186.
[54] S. W. Magennis, A. Habtemariam, O. Novakova, J. B. Henry, S. Meier, S. Parson, I. D. H. Oswald, V. Brabec, P. J. Sadler, *Inorg. Chem.* 46 (2007) 5059-5068.
[55] M. Melchart, A. Habtemariam, O. Novakova, S. A. Moggach, F. P. A. Fabbiani, S. Parsons, V. Brabec, P. J. Sadler, *Inorg. Chem.* 46 (2007) 8950-8962.
[56] K. E.; Erkkila, D. T.; Odom, J. K. Barton, *Chem. Rev.* 99 (1999) 2777-2796.
[57] H. Chao, W. J. Mei, Q. W. Huang, I. N. Ji, *J. Inorg. Biochem.* 92 (2002) 165-170.
[58] G. I. Cohen, W. R. Bauer, J. K. Barton, S. J. Lippard, *Science* 203 (1979) 1014-1018.
[59] S. E. Sherman, S. J. Lippard, *Chem. Rev.* 87 (1987) 1153-1181.
[60] L. Tjioe, A. Meininger, T. Joshi, L. Spiccia, B. Graham *Inorg. Chem.* 50 (2011), 4327-4339.

**Table 1:**

$IC_{50}$ (μM) Values Determined by MTT Assay after 72 h Exposure of the Compounds (**2a, 9a, 2b-4b and 8b-9b**) to the CRL7687 and CA-M75 cells

| Compounds | CRL7687[a] | CA-M75[b] |
|---|---|---|
| **2a** | 0.724 ± 0.2 | 0.852 ± 0.3 |
| **2b** | 0.724 ± 0.3 | 0.627 ± 0.4 |
| **3b** | 0.812 ± 0.4 | 0.946 ± 0.7 |
| **4b** | 0.892 ± 0.6 | 1.016 ± 0.9 |
| **9a** | 0.620 ± 0.1 | 0.613 ± 0.2 |
| **8b** | 0.688 ± 0.2 | 0.932 ± 0.5 |
| **9b** | 1.103 ± 0.8 | 19.70 ± 2.0 |

[a]Human melanoma cancer cells and [b]normal skin melanocytes

**CAPTIONS TO THE FIGURES:**

**Figure 1.** Time dependent UV-vis spectra of 30 μM **2b** (a) and **9b** (b) in PBS and 1% DMSO at 37 °C.

**Figure 2:** UV-vis absorption spectra of **2a** ($5.0 \times 10^{-5}$ M) in 5 mM Tris-HCl buffer (pH = 7.4) containing 50 mM NaCl in the presence of increasing amounts of CT-DNA (0-160 μM). Inset: the plot of $[DNA]/(\varepsilon_a-\varepsilon_f)$ vs. [DNA] for **2a**.

**Figure 3:** UV-vis absorption spectra of **2b** ($5.0 \times 10^{-5}$ M) in 5 mM Tris-HCl buffer (pH = 7.4) containing 50 mM NaCl and in the presence of increasing amounts of CT-DNA (0-160 μM). Inset: the plot of $[DNA]/(\varepsilon_a-\varepsilon_f)$ vs. [DNA] for **2b**.

**Figure 4:** Fluorescence emission spectra of **2a** ($1.0 \times 10^{-5}$ M) in 5 mM Tris-HCl buffer (pH = 7.4) containing 50 mM NaCl upon addition of increasing amounts CT-DNA (0-160 μM). Inset: the plot of $F/F_0$ vs. [DNA] for **2a**.

**Figure 5:** Fluorescence emission spectra of **2b** ($5.0 \times 10^{-6}$ M) in 5 mM Tris-HCl buffer (pH = 7.4) containing 50 mM NaCl upon addition of increasing amounts CT-DNA (0-160 μM). Inset: the plot of $F/F_0$ vs. [DNA] for **2b**.

**Figure 6:** Fluorescence emission spectra of EB bound to CT-DNA in the absence and presence of 0.0 – 80.0 μM **2a**, $\lambda_{ex}$ = 530 nm, DNA (40 μM), EB (4 μM) in 5 mM Tris-HCl buffer (pH = 7.4). Inset: the Stern-Volmer plot for quenching process of EB by **2a**.

**Figure 7:** Fluorescence emission spectra of EB bound to CT-DNA in the absence and presence of 0.0 – 80.0 µM **2b**, $\lambda_{ex}$ = 530 nm, DNA (40 µM), EB (4 µM) in 5 mM Tris-HCl buffer (pH = 7.4). Inset: the Stern-Volmer plot for quenching process of EB by **2b**.

**Figure 8.** Electrophoretic mobility patterns in agarose gel of pUC18 plasmid DNA treated with ligands **2a-4a** (lanes 2, 3 and 4) and ruthenium(II) complexes **2b-4b** (lanes 5, 6 and 7) for 2 h at 37 °C. Lane 1 is control DNA sample treated with TE buffer.

**FIGURES**

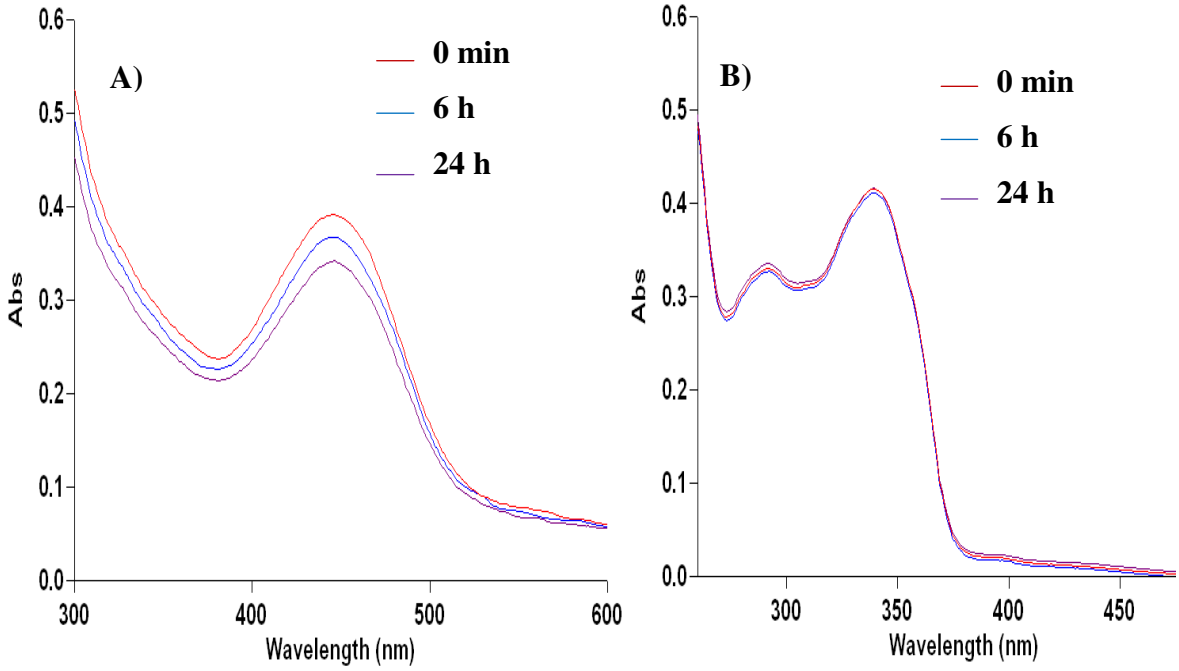


**Figure 1**

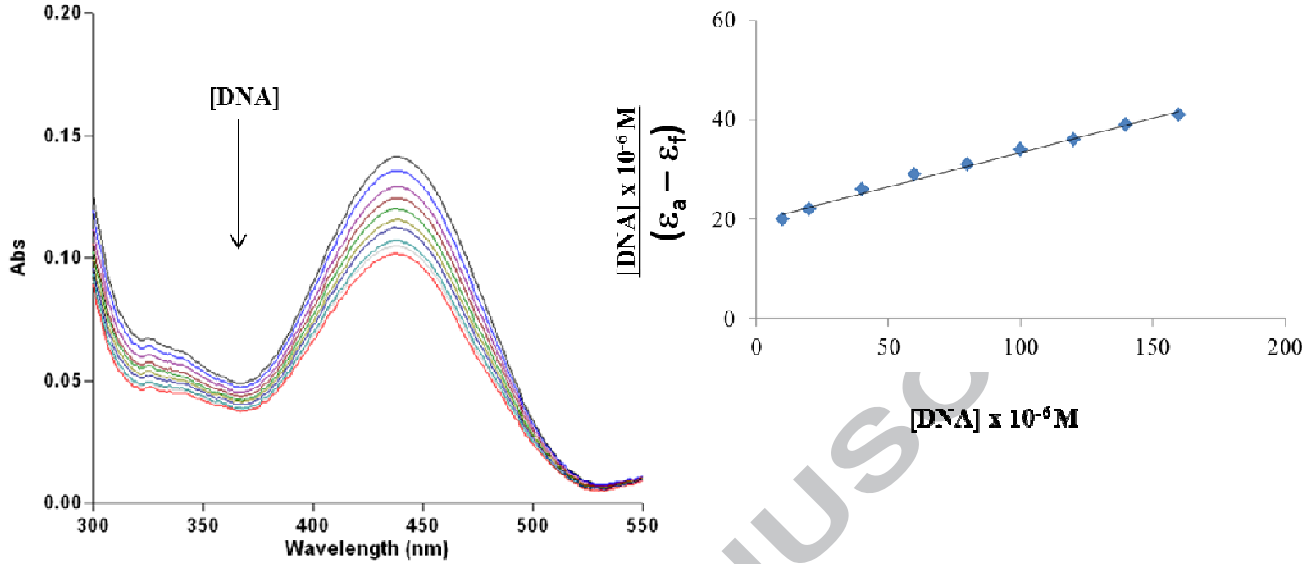


**Figure 2**

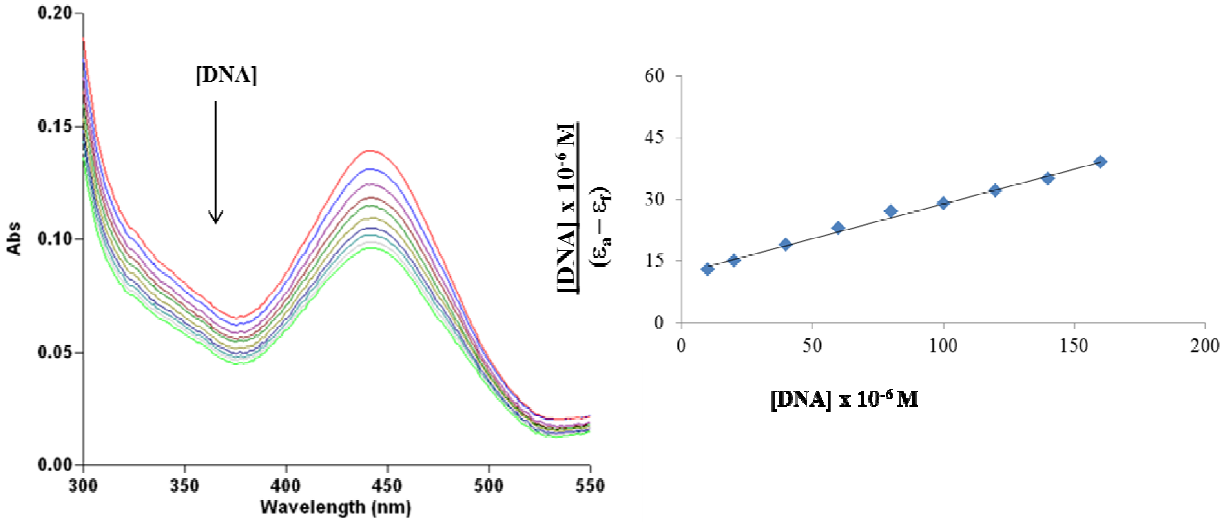


**Figure 3**

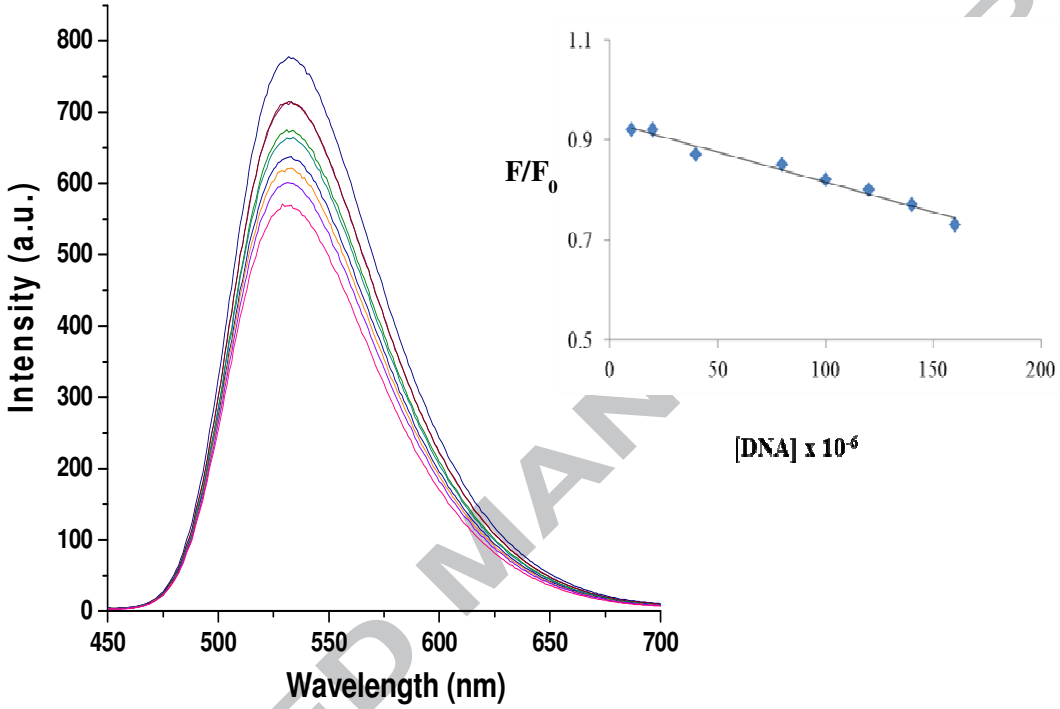


**Figure 4**

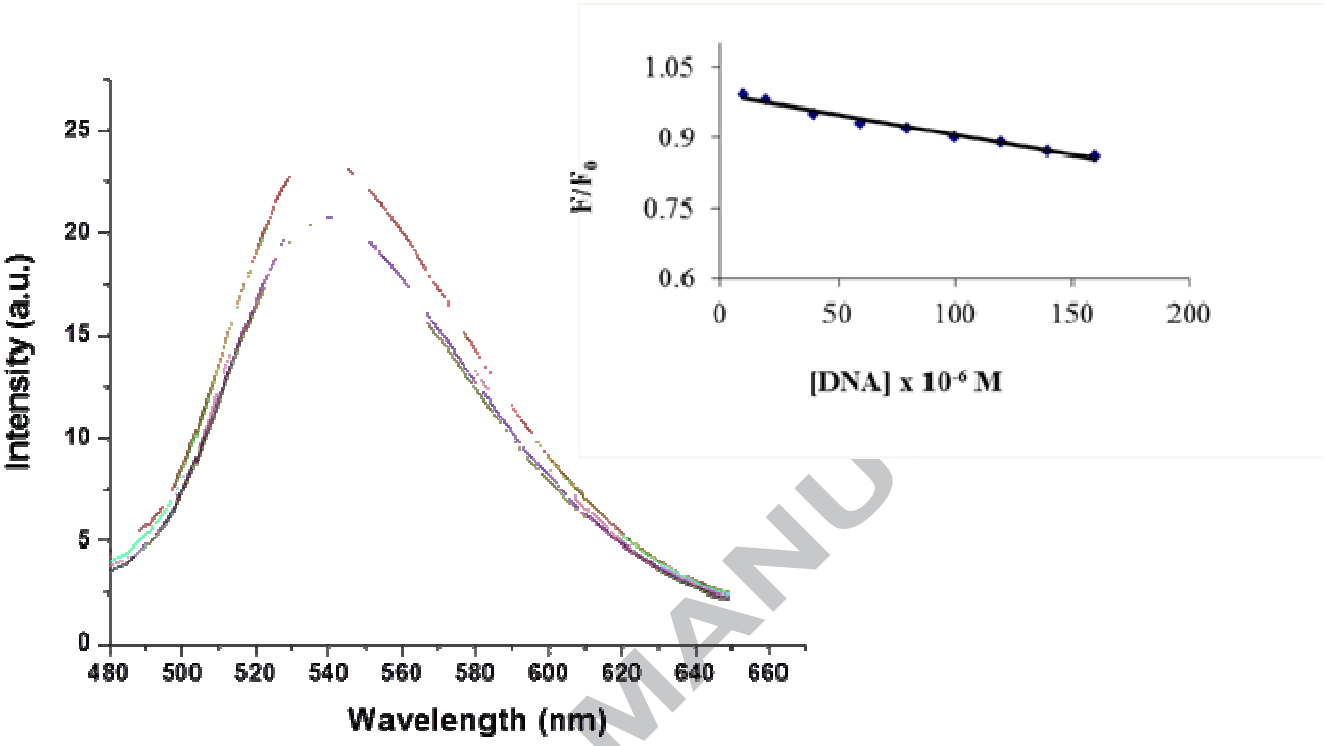


**Figure 5**

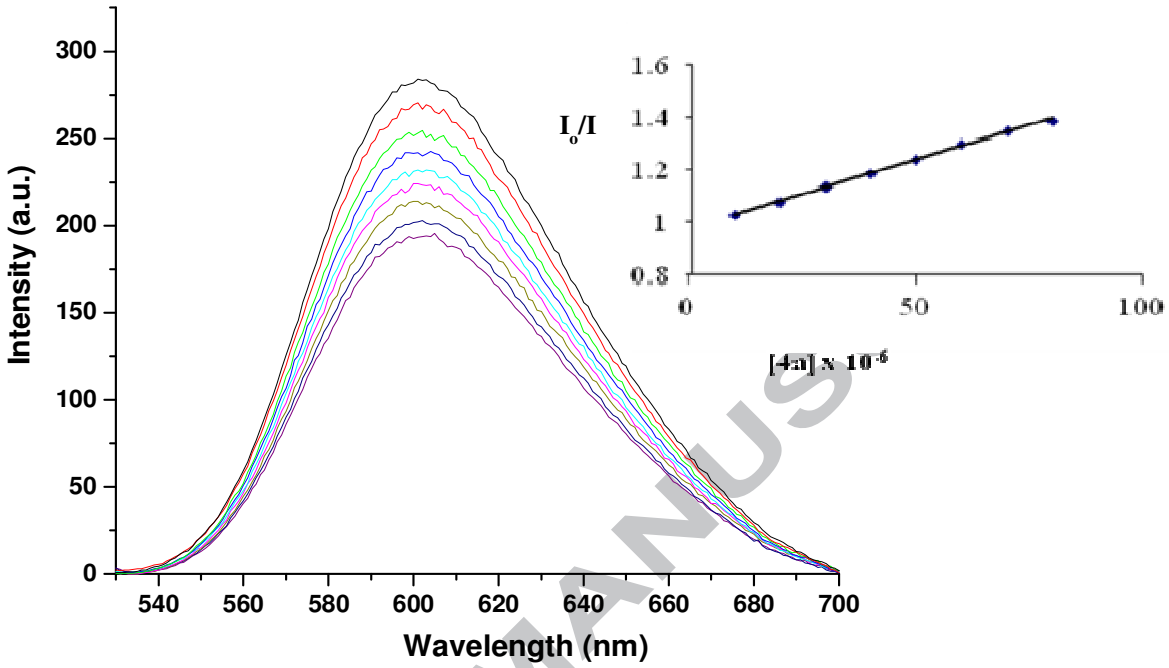


**Figure 6**

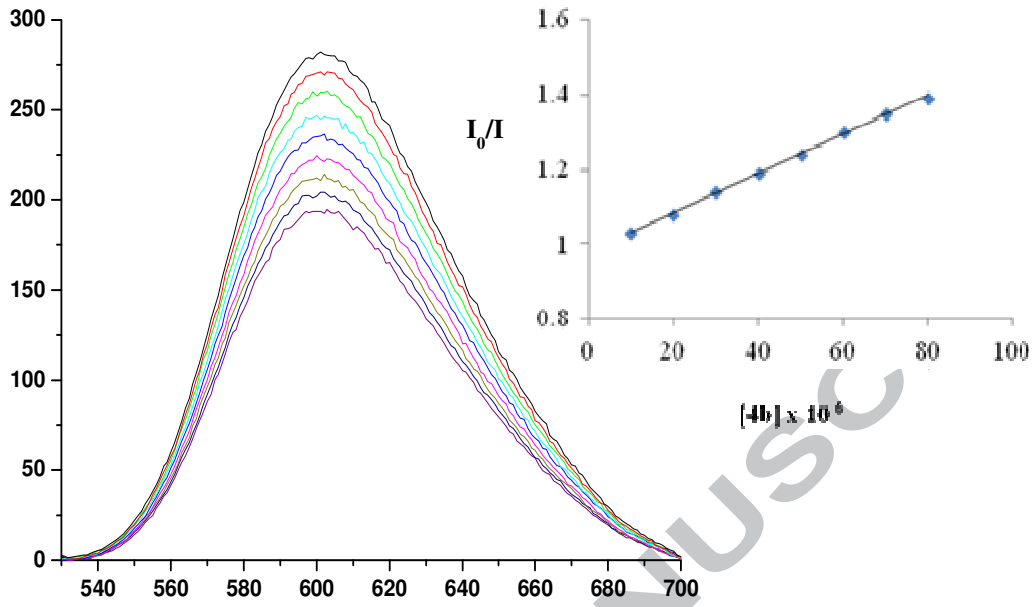


**Figure 7**

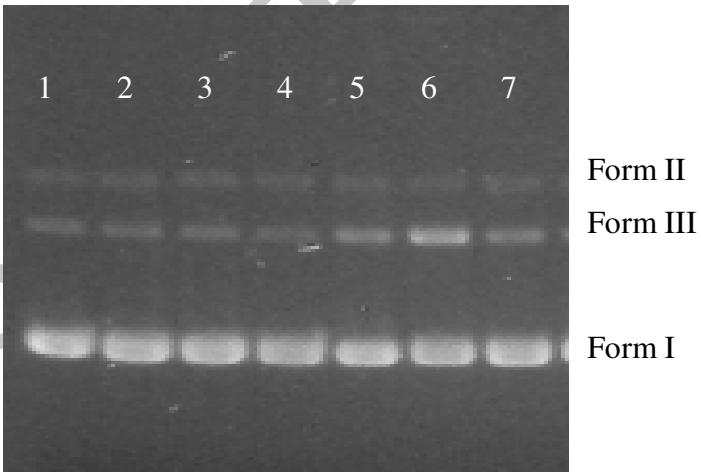


**Figure 8**

**SCHEMES**

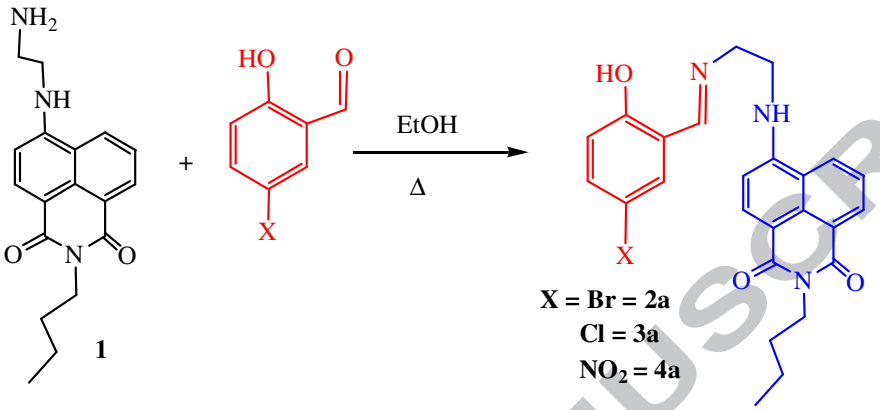


Scheme 1

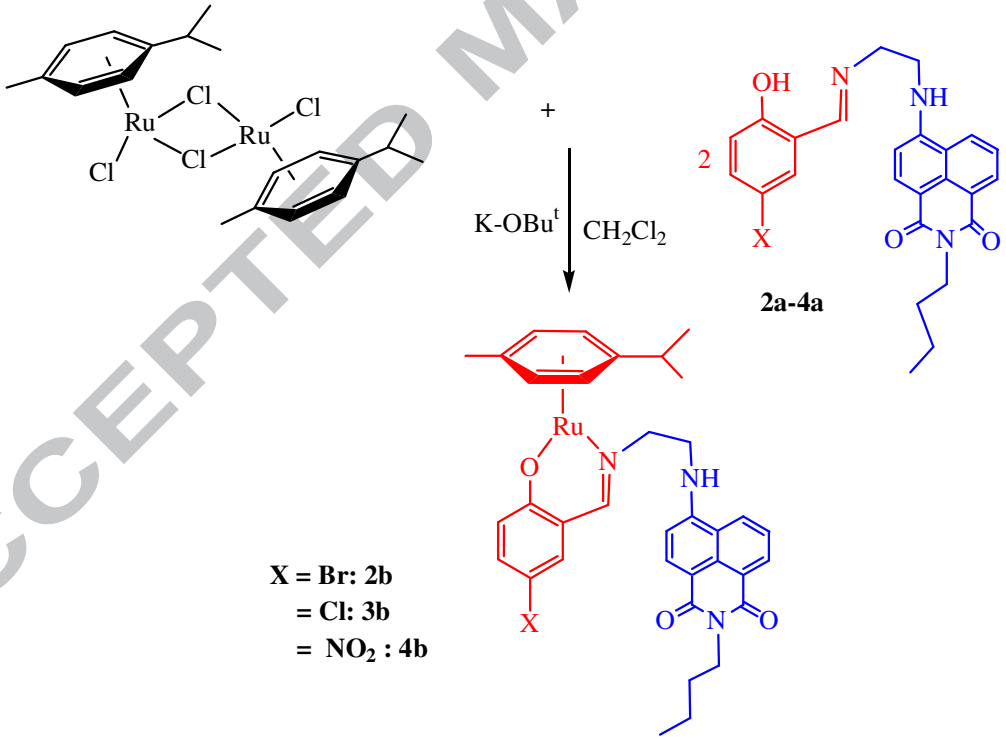


Scheme 2

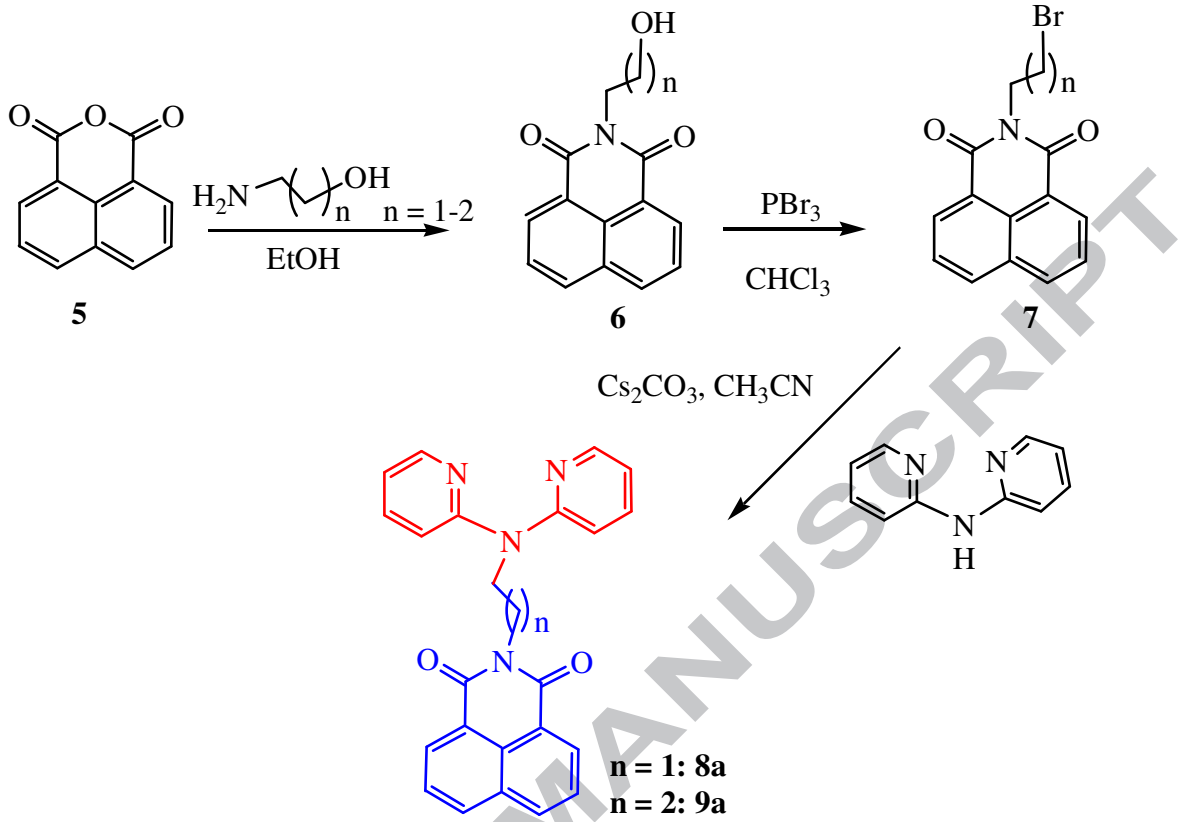


Scheme 3

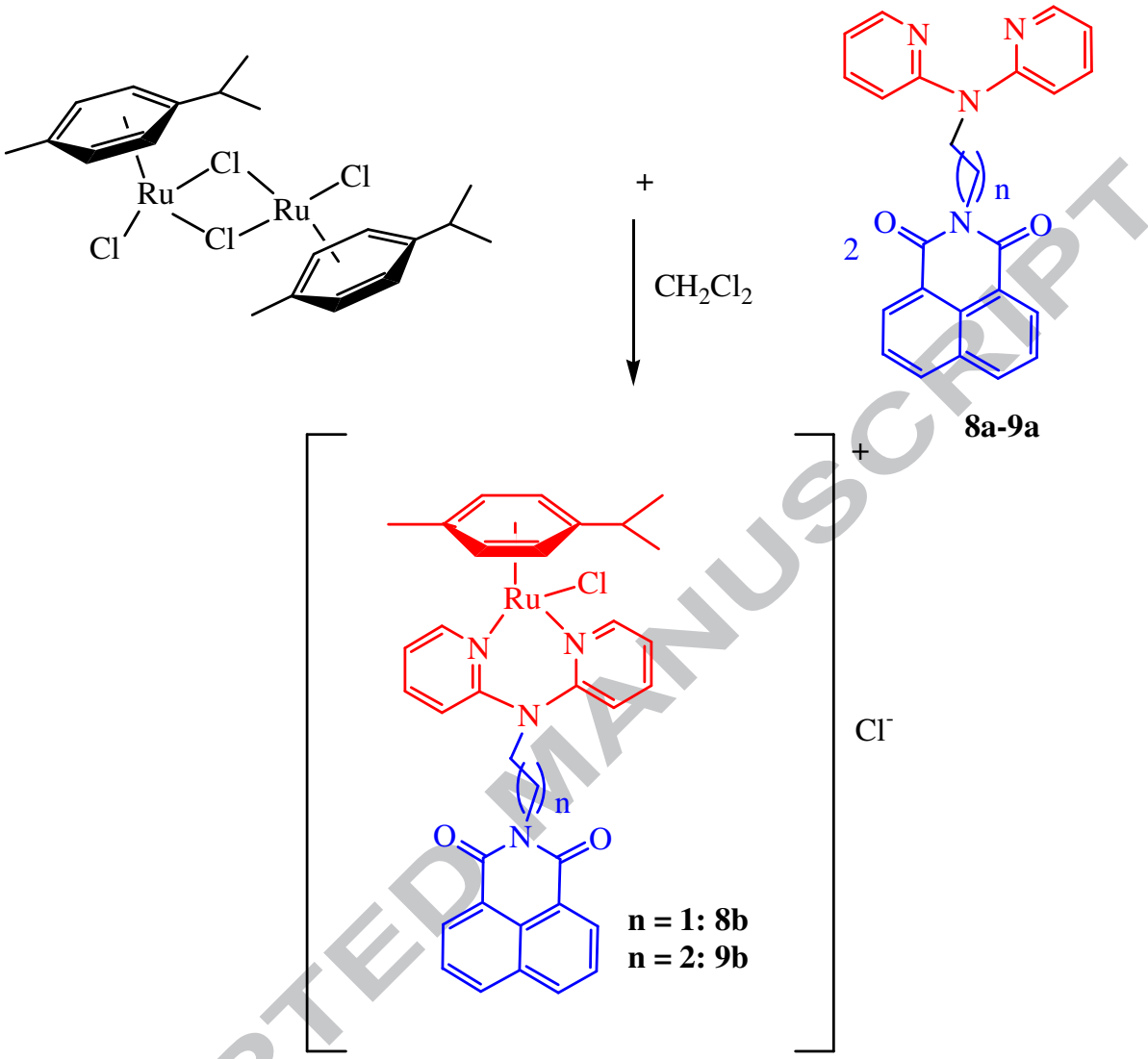


Scheme 4

**SYNOPSIS GRAPHICAL ABSTRACT**

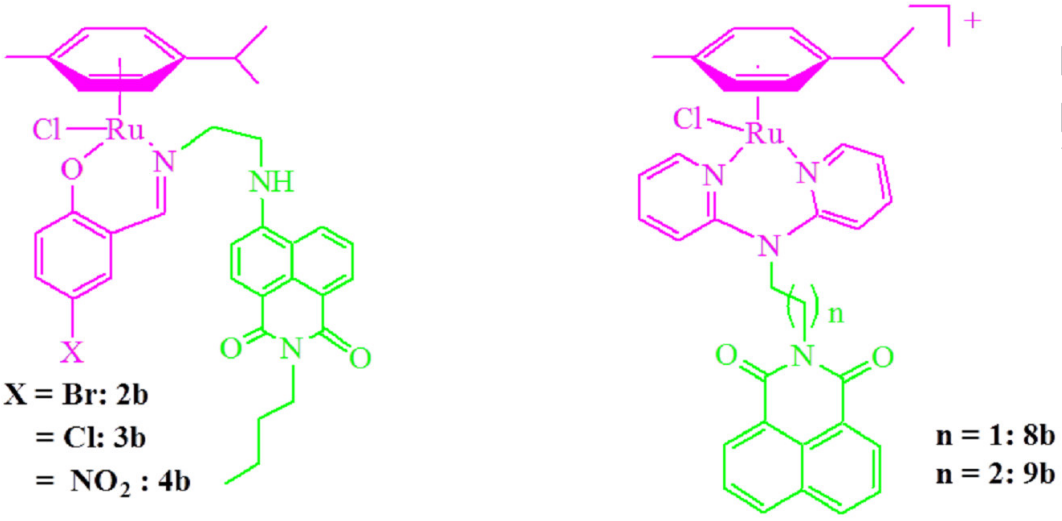


**Ruthenium(II)-Arene Complexes with Naphthalimide-Tagged N,O- and N, N-chelating Ligands: Synthesis and Biological Evaluation**

**HIGHLIGHTS**

- Synthesis of new ruthenium(II)-arene complexes using naphthalimide–tagged N, O- and N, N-based chelating ligands

- Cytotoxic activity against cancerous and normal cell lines.

- DNA-binding Studies

- Influence of the naphthalimide chromophore and intercalating agent on cytotoxicity and DNA-binding

- Influence of chain length and substituents on cytotoxicity and DNA-binding

**Supporting Information for**

# Ruthenium(II)-Arene Complexes with Naphthalimide-Tagged N,O- and N, N-Chelating Ligands: Synthesis and Biological Evaluations

Kesete Ghebreyessus[a]* Ashley Peralta[a#], Meena Katdare[b] Krishnan Prabhakaran[b#], Shanthi Paranawithana[a],

[a]Department of Chemistry ; and [b] Skin of Color Research Institute, Hampton University, Hampton, VA 23668

[a]* Corresponding Author: Prof. Kesete Ghebreyessus, Department of Chemistry, Hampton University, Hampton, VA 23666, USA.

E-mail: Kesete.Ghebreyessus@hamptonu.edu. Telephone: +1-757-727-5475

Fax:+1-757-727-5604

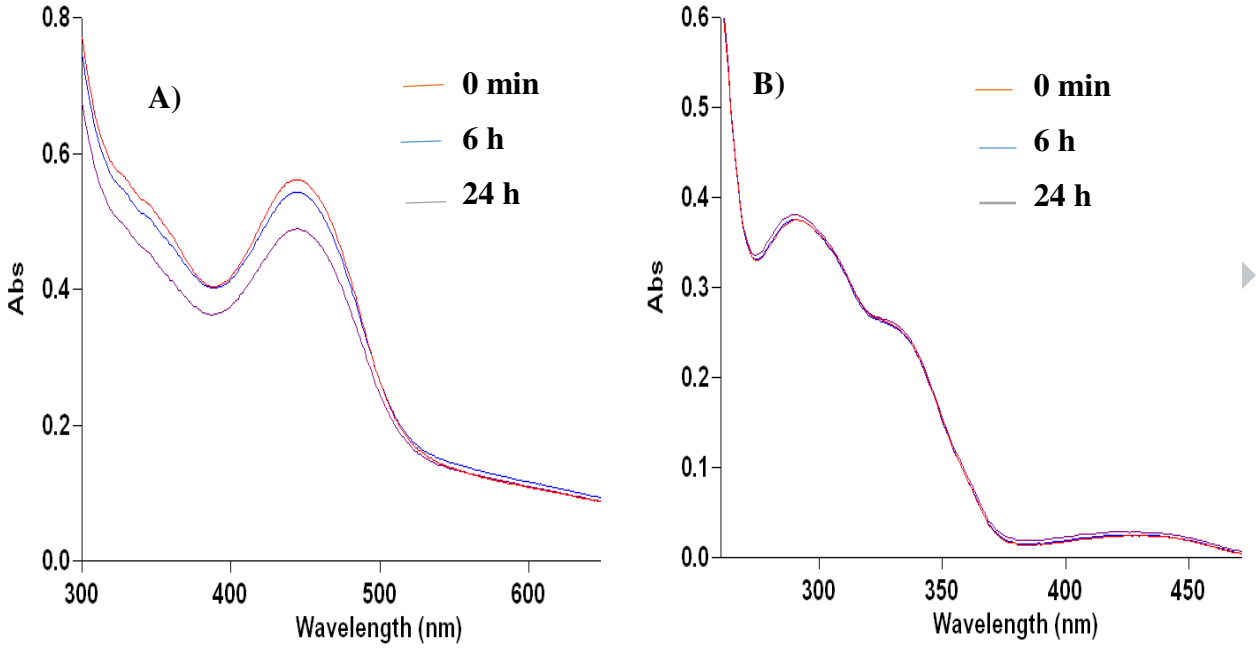


**Figure S1.** Time dependent UV-vis spectra of 30 µM **3b** (a) and **8b** (b) in PBS and 1% DMSO at 37 °C.

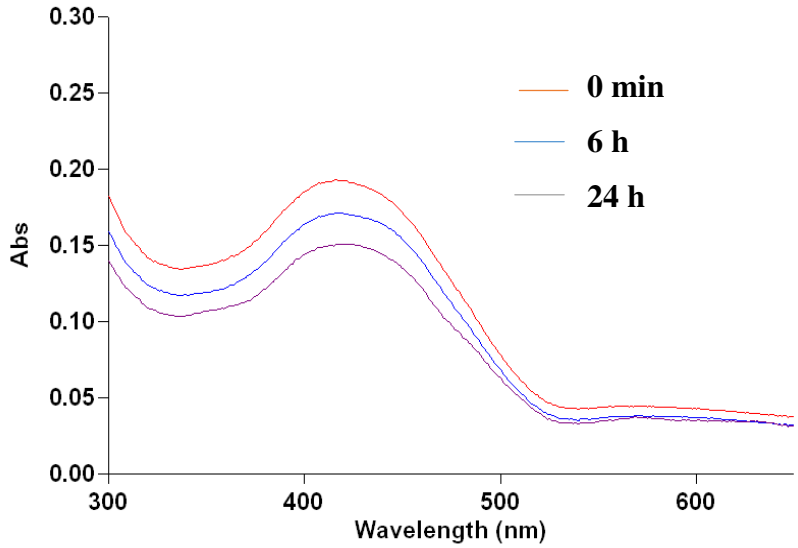


**Figure S2.** Time dependent UV-vis spectra of 30 µM **4b** in PBS and 1% DMSO at 37°C.

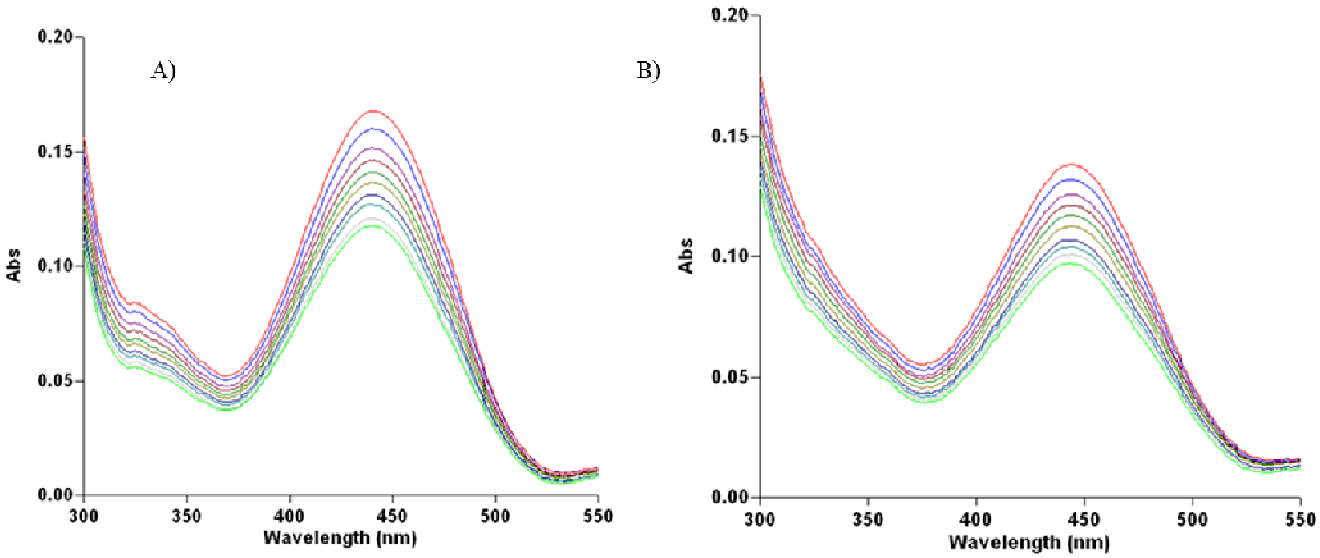


**Figure S3.** UV-vis absorption spectra of **3a** (a) and **3b** (b) ($5.0 \times 10^{-5}$ M) in 5 mM Tris-HCl buffer (pH = 7.4) containing 50 mM NaCl in the presence of increasing amounts of CT-DNA (0-160 μM).

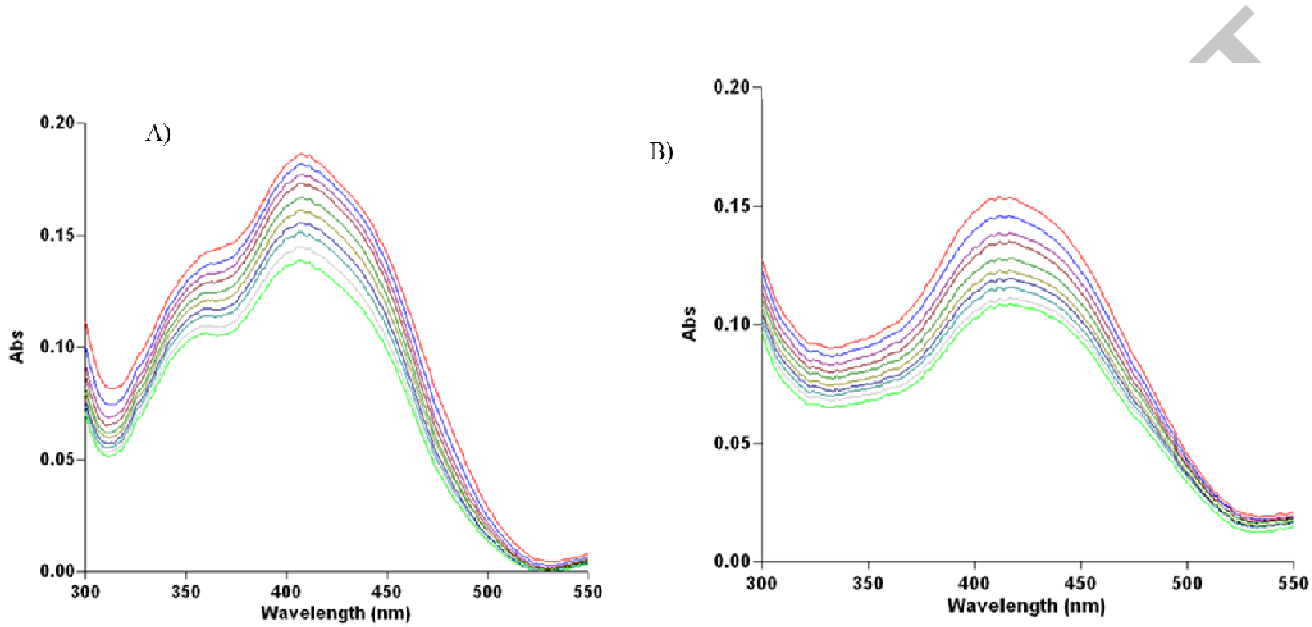


**Figure S4.** UV-vis absorption spectra of **4a** (a) and **4b** (b) ($5.0 \times 10^{-5}$ M) in 5 mM Tris-HCl buffer (pH = 7.4) containing 50 mM NaCl in the presence of increasing amounts of CT-DNA (0-160 µM).

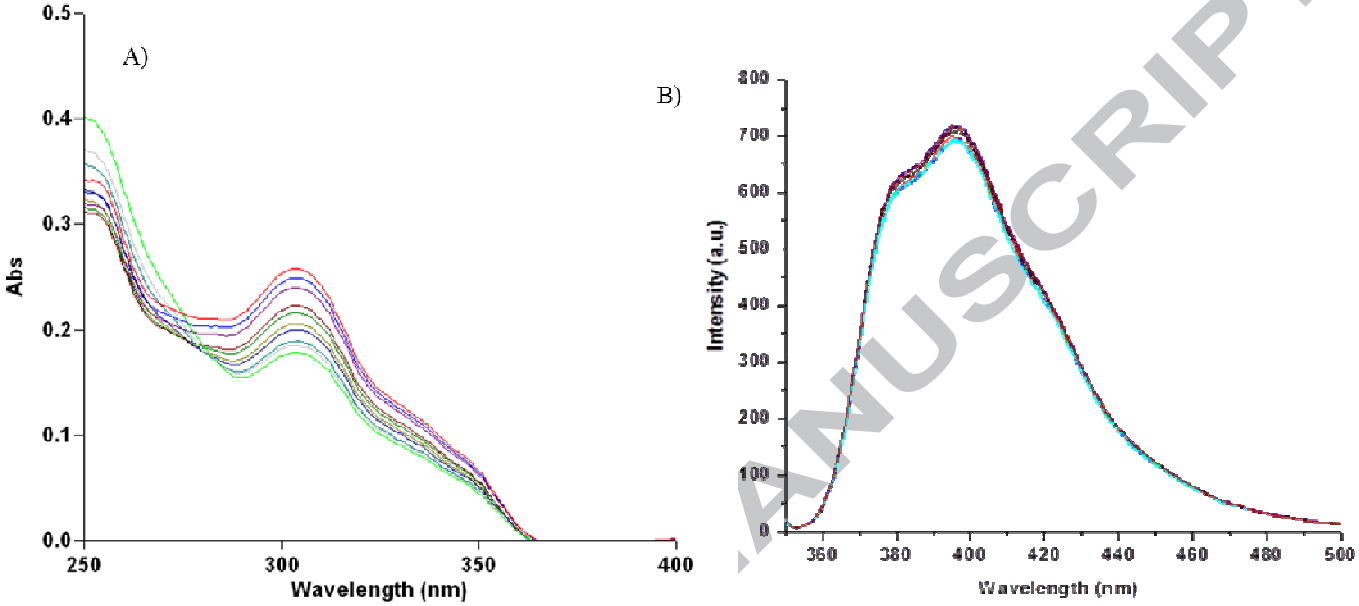


**Figure S5.** a) UV-vis absorption spectra of **8a** ($5.0 \times 10^{-5}$ M) in 5 mM Tris-HCl buffer (pH = 7.4) containing 50 mM NaCl in the presence of increasing amounts of CT-DNA (0-160 µM). b) Fluorescence emission spectra of **8a** ($5.0 \times 10^{-5}$ M) in 5 mM Tris-HCl buffer (pH = 7.4) in the presence of CT-DNA (0.0-80 µM).

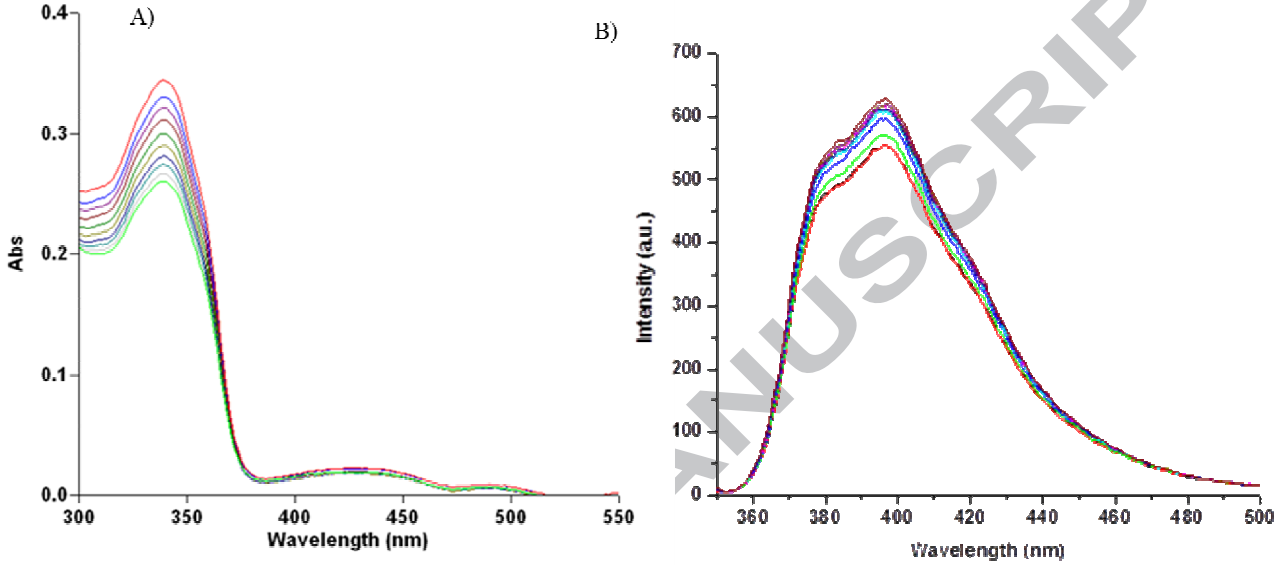


**Figure S6.** a) UV-vis absorption spectra of **8b** ($5.0 \times 10^{-5}$ M) in 5 mM Tris-HCl buffer (pH = 7.4) containing 50 mM NaCl in the presence of increasing amounts of CT-DNA (0-160 µM). b) Fluorescence emission spectra of **8b** ($5.0 \times 10^{-5}$ M) in 5 mM Tris-HCl buffer (pH = 7.4) in the presence of CT-DNA (0.0-160 µM).

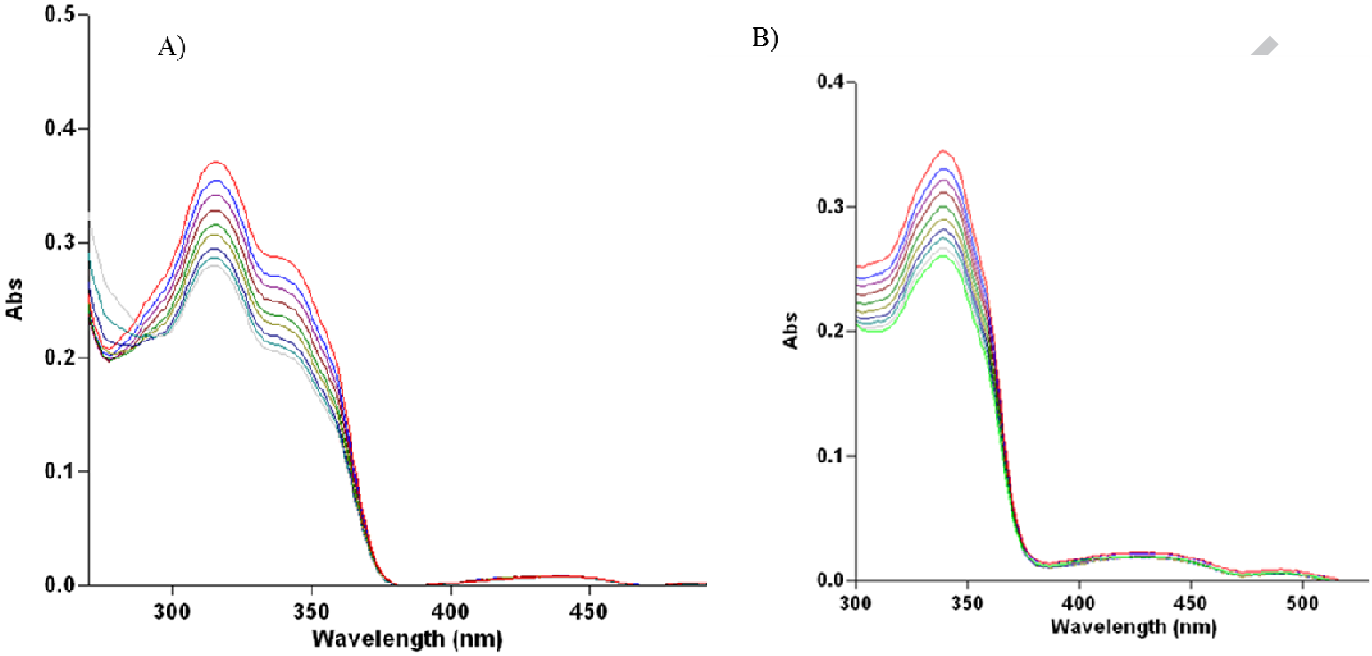


**Figure S7.** UV-vis absorption spectra of **9a** (a) and **9b** (b) ($5.0 \times 10^{-5}$ M) in 5 mM Tris-HCl buffer (pH = 7.4) containing 50 mM NaCl in the presence of increasing amounts of CT-DNA (0-160 µM).

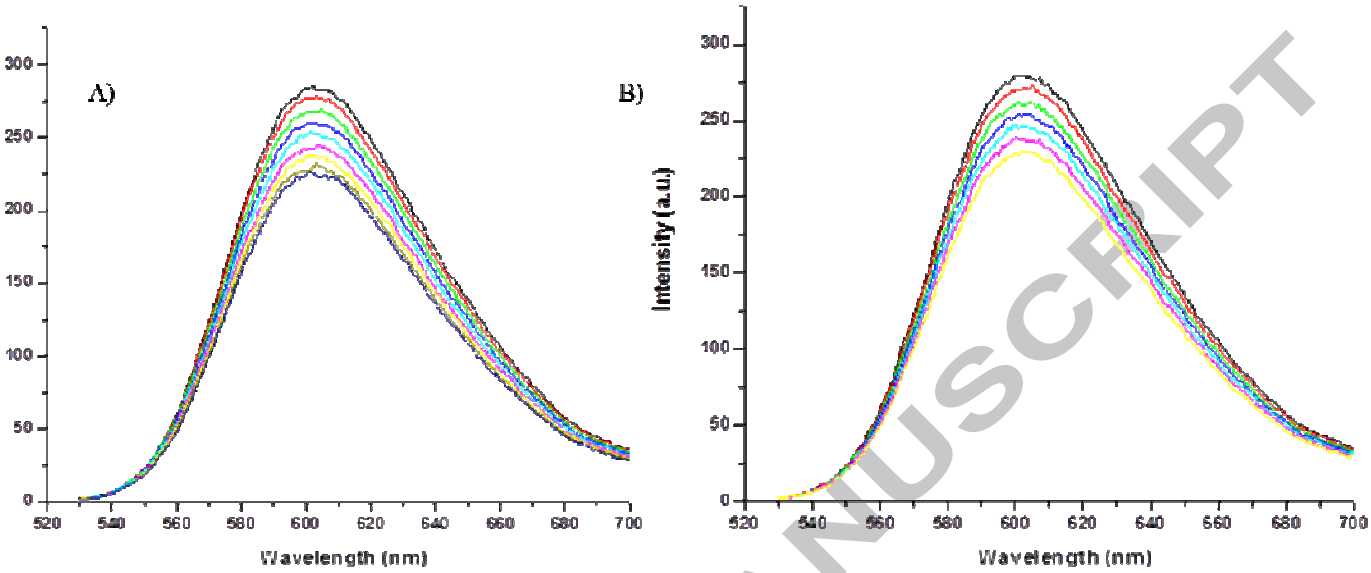


**Figure S8.** a) Fluorescence emission spectra of EB bound to CT-DNA in the absence and presence of 0.0 – 50.0 µM **8a**, $\lambda_{ex}$ = 530 nm, CT-DNA (40 µM), EB (4 µM) in 5 mM Tris-HCl buffer (pH = 7.4). b) Fluorescence emission spectra of EB bound to DNA in the absence and presence of 0.0 – 50.0 µM **8b**, $\lambda_{ex}$ = 530 nm, CT-DNA (40 µM), EB (4 µM) in 5 mM Tris-HCl buffer (pH = 7.4).